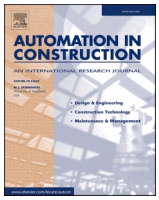
Automation in Construction 162 (2024) 105390



Contents lists available at ScienceDirect

Automation in Construction

journal homepage: www.elsevier.com/locate/autcon





Enhanced co-design and evaluation of a collective robotic construction system for the assembly of large-scale in-plane timber structures

Samuel Leder [a,e,1,*], HyunGyu Kim [b,e,1], Metin Sitti [b,c,d,e,**], Achim Menges [a,e]

[a] Institute for Computational Design and Construction (ICD), University of Stuttgart, Keplerstrasse 11, Sttutgart 70174, Germany
[b] Physical Intelligence Department, Max Planck Institute for Intelligent Systems, Heisenbergstraße 3, Stuttgart 70569, Germany
[c] Institute for Biomedical Engineering, ETH Zurich, 8092 Zurich, Switzerland
[d] School of Medicine and College of Engineering, Koç University, 34450 Istanbul, Türkiye
[e] Cluster of Excellence Integrative Computational Design and Construction for Architecture (IntCDC), University of Stuttgart and Max Planck Institute for Intelligent Systems, Germany, Stuttgart, Germany

ARTICLE INFO

Keywords:
Collective robotic construction
Mobile robotics
Architecture
Construction automation
Mechatronics

ABSTRACT

Collective robotic construction (CRC) is an emerging approach to construction automation based on the collaboration among teams of small mobile robots. This paper enhances an existing modular CRC system, showcasing its capability to assemble full-scale in-plane timber structures. Utilizing strategies of co-design, the robotic actuators were updated to accommodate material tolerance in the passive building material, timber struts, which they use for locomotion and assemble into structures. A custom effector was also developed to establish architecturally relevant, structural connections between struts. The enhancements address two major challenges in CRC system development: material tolerance and connections. To showcase these research findings and compare with other construction automation systems, a reinforced slab structure was assembled. With a building envelop of 0.485 m^3, this is one of the largest structures assembled by a CRC system. As such, the work highlights the potential applicability of CRC in real-world architectural projects.

1. Introduction

Due to the promise of increased productivity, efficiency and economic performance, there is an growing interest in the automation of construction since its origins in the early 1970s [1]. As such, there have been various approaches to the automation of construction that have been developed over the years. What began as a series of experiments on off-site building component manufacturing and large-scale prefabrication, gradually expanded towards the automation of heavy-duty construction equipment and the investigation of on-site robotic fabrication factories. A more recent approach to construction automation is collective robotic construction (CRC) in which a swarm or team of mobile robots collaborate in the construction process [2]. The major goal of research in CRC is the development or application of simple machines for the assembly of structures that greatly surpass the size of the machines themselves. Although the robots are generally small in size especially as compared to other approaches to construction automation, research in the field of CRC has been continuously growing since initial experiments in the 1990s.

A pivotal factor driving the ongoing research in CRC is the size and simplicity of the robots. As the small size of the robots makes CRC systems generally easy to transport, they can be moved around for both on- and off-site construction automation. The limited set up required of the robots further allows CRC systems to be deployed regardless of site conditions. The low cost of a single robot also means more robots can be added to increase the speed of assembly or if one breaks then it can be replaced by another. Furthermore, the mobile and lightweight nature of the robots allows them to climb through or over a structure, breaking the reach restriction of fixed positioning robots and allowing them to inhabit the structure for repair, maintenance or adaptation.

However, the size of the robots creates some challenges for CRC. For example, due to their compactness, the robots tend to have low payloads meaning that the size and weight of the material they can transport is relatively low. Additionally their ability to assemble materials that

* Corresponding author at: Institute for Computational Design and Construction (ICD), University of Stuttgart, Keplerstrasse 11, Sttutgart 70174, Germany.
** Corresponding author at: Physical Intelligence Department, Max Planck Institute for Intelligent Systems, Heisenbergstraße 3, Stuttgart 70569, Germany.
E-mail addresses: samuel.leder@icd.uni-stuttgart.de (S. Leder), sitti@is.mpg.de (M. Sitti).
[1] These authors contributed equally to this publication.

https://doi.org/10.1016/j.autcon.2024.105390
Received 20 July 2023; Received in revised form 22 February 2024; Accepted 12 March 2024
Available online 22 March 2024
0926-5805/© 2024 The Author(s). Published by Elsevier B.V. This is an open access article under the CC BY-NC license (http://creativecommons.org/licenses/by-nc/4.0/).

require high force to make connections is limited. This poses a problem when attempting to assemble full-scale building projects. Moreover, a substantial amount of research in CRC is conducted in simulation based on principles of self-organization. The majority of research is conducted in simulation because CRC largely stems from the field of distributed computing [3–6]. Many simulations ignore real kinematic constraints or use simulant materials as placeholders in their digital investigations.

Research on CRC is however beginning to include developments on physical robots assembling structures in the real world, which has seen a transition due to more advanced hardware and sensing technologies. Specifically, initial, highly experimental explorations at a limited scale using custom building blocks [7–9] are transitioning to in-depth experiments with real-world building materials assembled into spatial structures [10,11]. This transition has meant that the additional practical challenges of real-world construction are becoming more important to the development of CRC systems and the ability to evaluate such systems against existing approaches to automation in construction is becoming more feasible.

1.1. Aim and research question

Despite the growing interest in CRC, there is still a limited amount of research focusing on CRC utilizing conventional building materials that are common in current building projects. This highlights the need for further investigation, particularly when considering the application of CRC in full building scale projects. The primary objective of this paper is twofold. Firstly, it aims to present an advanced co-design of a CRC system, as previously introduced by Leder et al. [12]. This co-design specifically considers the assembly of an in-plane timber structure, meaning the timber elements are assembled in the same plane, and explores the potential of CRC in this context. Secondly, the paper seeks to evaluate the proposed CRC system as an alternative approach to automation in the construction industry, compared to larger scale machinery.

While previous research has introduced the system and demonstrated the capabilities of the robotic system in performing construction tasks required for eventual structure assembly [12], this paper takes a step further by fully assembling a large-scale in-plane timber building prototype (Fig. 1). Initial attempts at the assembly were met with two significant physical challenges that are commonly encountered in CRC research: (i) material tolerances, relating to the inaccuracy in machining of materials, and (ii) material connections, relating to the insertion of structurally stable connections between building material as a structure is assembled. To address these challenges, further mechatronic co-design, testing and performance evaluation of the robotic hardware in the proposed system were performed in order to deal with tolerances in the timber building material and enable the robot to mechanically fasten the timber. The results of these developments were integrated into the overall CRC system. The co-design process behind this are discussed within this paper together with a report on the assembly of the prototype in Fig. 1.

Furthermore, an evaluation of the assembly was conducted, comparing the proposed system to other forms of automation in timber construction and CRC. In detailing such, the aim of this research is to not only validate the effectiveness of CRC systems but also critically analyze their potential impact on the construction industry. The final prototype of this research is one of the largest assembled structures assembled by a CRC system. Through this research, the aim is to highlight the significance and relevance of CRC, providing valuable insights into addressing problems when dealing with such automation systems and aid in the further development and eventual wider adoption of CRC in future building projects.

2. Context and related work

This research is situated in the context of CRC as well as in automation in timber construction. Automation in timber construction is important to this research as it serves as a backdrop for the evaluation of the presented CRC system.

2.1. Collective robotic construction (CRC)

Research in the development of physical CRC systems is diverse in the range of approaches from application scenarios to assembly and planning algorithms implemented. Two parameters that highly affect the development and demonstrate the range of CRC systems are the robot system and the material system. The range of CRC research based on these two parameters has included ground [10,13–15] [16,17], aerial [9,18] and water vehicles [19] as well as robots which can only locomote on the structure they build [11] on the side of the robot and custom bricks [14,20,21], struts [12,22,23] and fibers [18,24] as some of the many explored options on the side of the material. Some research also conflates the material and robot in which the building elements are mechanized into robots in order to allow for continuous adaptation or rearrangement [25,26]. Although the choice of material and robot have tradeoffs in terms of the ability and construction outputs of the entire

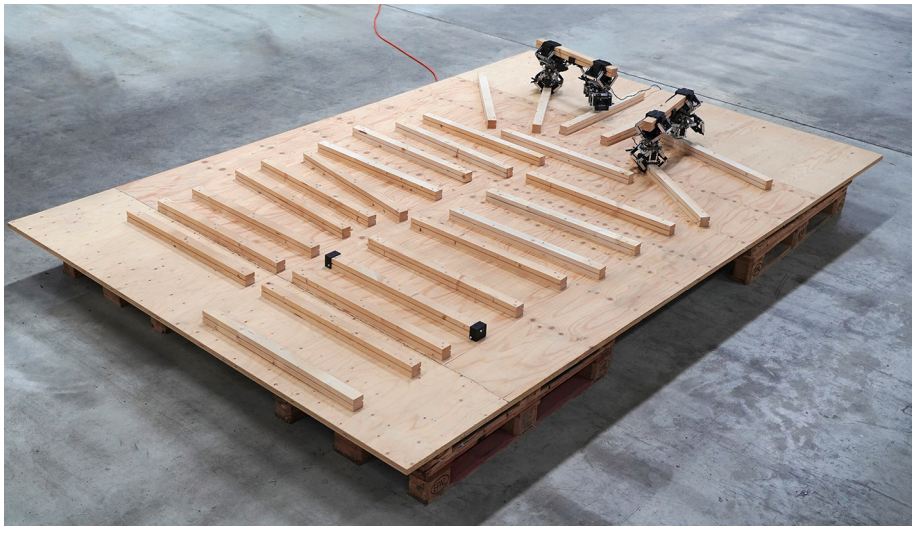


Fig. 1. Photograph of a large-scale in-plane building prototype assembled by a custom CRC system of modular robotic actuators and timber struts. 25 spruce timber struts of dimension 50 mm by 50 mm by 850 mm are connected via screws to a plywood timber sheet of dimension 3880 mm by 2500 mm.

CRC system, two challenges regardless of the material or robot in research on physical CRC systems are: (i) material tolerance and (ii) material connections.

Dealing with material tolerances is an important factor in the development of CRC. Material tolerances in construction automation can relate (i) to incorrectly attaching material to the existing structure causing deviation in the assembly process or (ii) to the handling of deviations in materials themselves. In the first case, although CRC systems are seen as robust as one machine can replace another, the potential for errors multiply due to the larger amount of machines that are working together [27]. Large buildup of error can block the robots from working on the structure or cause instability of the structure being assembled. In order to understand the impact of error propagation, research from Chen et al. is exploring the effects of error on collective construction [28]. They also propose methods for error mitigation using local checks using sensor feedback to evaluate successful steps in the assembly process [28]. Other research deals with the handling of error relating to the assembly of material using various sensor feedback loops [9,14,29,30].

However, in all of this research the material is custom building material, ignoring the chance for variation in manufacturing that occurs in real building material. In this research, material tolerances refers to dealing with the variation from specified dimensions that occur through the manufacturing of the material. This is an important factor because building elements that are fabricated out of tolerance are a major source of problem or failures in general construction [31] and in construction with robotics, more specifically [32]. If the robots are not able to account for tolerances in machining, there is a high chance for additional errors in the assembly process. Such errors include deviations from the planned structure and, in extreme cases, may result in the complete termination of the assembly process, as in the case when a robot drops material where others robots need to locomote in order to continue the assembly process.

To answer this in CRC, co-design of a material together with the robotic system has been utilized as a means of standardizing the interaction between the material and robotic agents [23,30]. The robotic system can self-align to the material. However, this mostly results in highly customized building materials otherwise not present or applicable in construction. To the best of our knowledge, the notion of co-design between the material and robot has not been extended to materials currently present in the building industry. Therefore, this paper builds upon our previous work [12] to further co-design of the mobile robot to deal with material tolerance in the pre-fabrication of timber building materials.

The second challenge in CRC dealt with in this paper is material connections. Within any type of construction, the connections between building material are what holds a structure together and are of importance to the stability as well as the range of architectural design of the structure. Inserting or performing a connection, however, can be a complex construction task that can demand high force and potentially further require custom mechanisms to be achieved. Therefore, research on CRC often attempts to simplify this part of the system to keep an overall low level of complexity across the entire system. Some research on CRC systems addresses the question of connection by utilizing amorphous or compliant materials, meaning the connections are a product of the assembly process itself. For example, foam has been utilized in consecutive spraying processes, allowing for the material to harden on itself and build up a structure through such a process [15,16]. Research dealing with discrete materials has addressed the question of connections in a variety of ways. This has included (i) utilizing non-structural connections such a magnet [9,30], (ii) developing systems for the dry stacking of building elements [10,20] and in some cases (iii) relying on the insertion of connections through external intervention [23]. Although each are viable options for advancing research, they have considerable limitations when considering the autonomy, architectural geometric freedom and structural viability of CRC systems.

2.2. Research on automation in timber construction

Although there is a long-standing history of timber construction, the utilization of timber as a building material has fluctuated over time, particularly in comparison to other materials [33]. Towards the end of the 20th century, the advent of engineered wood products facilitated a reconsideration of timber as a construction material for diverse building projects [34]. With their manufacturing now fully automated, engineered wood products are enabling architects and engineers across the globe to design and build timber buildings.

However, despite ongoing advancements in research on timber construction, engineered wood products currently do not completely match the strength and stiffness of other construction materials such as steel or concrete. Considering this, there is also a requirement to innovate on timber building systems on top of the timber products from which they are assembled [35]. Various academic research institutions are thus developing new timber building systems in which geometry serves as a driver for making structures that are more complex, reach longer spans, and achieve new heights [36]. Research from Gramazio Kohler Research at ETH Zürich has showcased a range of complex spatial assemblies [37], as well as bespoke timber frames made out of linear timber building elements [38]. Research at the Cluster of Excellence Integrative Computational Design and Construction for Architecture (IntCDC) is also currently investigating new timber building systems for multi-storey buildings. One part of this research are slab typologies that are reinforced with timber beams according to the structural layout of the entire structure [39,40]. Fig. 2 is a representation of a hollow box slab that is currently being researched. The design of the slab is based on force flow [41]. The structure assembled in this research involves the placement of linear timber beams on a timber plate, similar to the slabs being developed in the IntCDC.

The exploration of these new building systems is enabled not only by advancements in timber products and the automation of their manufacturing, but in many cases, it is also due to the affordances of robotic technologies. Research is currently being conducted on the utilization of different robotic setups for timber assembly. The setups include different amounts, types, and scales of robots. The largest assembly from Gramazio Kohler Research was fabricated using a six-axis overhead gantry robot, developed at ERNE Holzbau AG in collaboration with ROB Technologies AG [37]. The various slab morphologies that are being developed at the IntCDC have been assembled using different robot setups, specifically a robotic platform called TIM with two industrial KUKA robotic arms [42] and an industrial robot arm on top of a track vehicle [39]. Recent research from Leung et al. (2019) has also introduced small-scale robotic clamps to aid in timber frame assembly [43,44]. The large motions of the timber building elements are made by an industrial robotic arm. The clamps, therefore, only provide

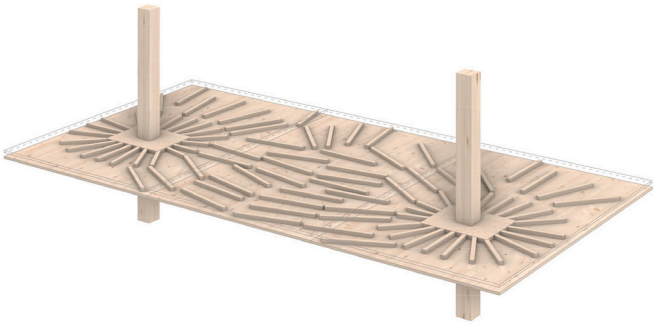


Fig. 2. Diagrammatic representation of hollow box slab being developed in the IntCDC [40]. The slab is composed of a top and bottom plate which sandwich linear timber beams and additional timber elements for the connection of columns to the slab. The top plate is outlined in grey dashed lines to be able to see the interior of the slab.

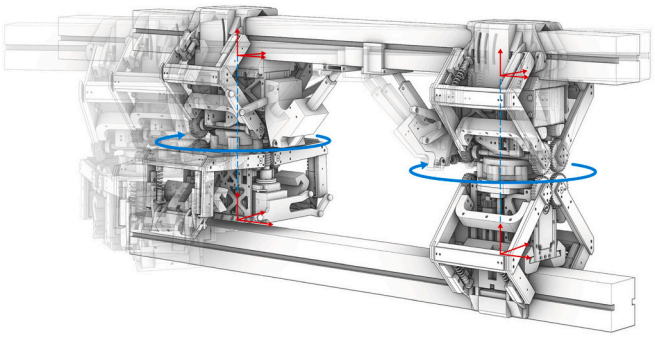


Fig. 3. Kinematic description of kinematic chain with two robotic actuators. Each robotic actuator has a rotational degree of freedom (DOF), which when combined allow for mobility in the CRC system. The curved blue arrows and dashed blue lines indicate the DOF for each robotic actuators. The straight red arrows indicate the planes at which each robotic actuator can attach to a passive strut. (For interpretation of the references to colour in this figure legend, the reader is referred to the web version of this article.)

force to help with the tight-fit connections in the frames being assembled. In terms of scale, this paper presents the robotic system with the smallest known machines that are capable of autonomously assembling timber structures.

2.3. Performance metrics for automation in construction

Even though there are many years of research on automation and robotics in construction, the adoption of such technology in industry remains low. It is reported that the major reasons behind this are economical and technical as well as the value of construction automation still not being understood [45]. To clarify the value, there has been some recent effort to develop metrics to help evaluate different approaches to automation in construction. In 2018, for example, Pan et al. developed a framework for assessing construction automation and robotics in the context of sustainability [46]. The framework contains four major categories, including: (i) environmental, (ii) economic, (iii) social and (iv) technical, as well as many sub-categories for each. Although useful in giving an overview of how to assess approaches to automation in construction, such discussions are left at a high level with no specifics on how to quantifiably or qualitatively use the metrics.

It is difficult to make universal benchmarks for comparison and assessment of automation in construction because of the multitude of different approaches that exist. Therefore, reports of research tend to evaluate their developments in isolation from other approaches. One exception to this is in the research on the digital construction platform (DCP). In the reporting of the research on DCP, comparison of the DCP is made with existing automated construction research with both quantitative and qualitative metrics [47]. The three quantitative metrics are (i) the largest fabricated structure, (ii) the total work volume and (iii) volumetric fabrication rate. Although they do recognize the limitation of their metrics to cover all points of comparison, a similar approach will be taken in this paper of using both qualitative and quantitative metrics to assess the proposed system.

Within the field of CRC specifically, the discussion of performance metrics and their importance was introduced by a review paper on the topic of CRC by Petersen et al. [2]. The authors list major factors for benchmarking different approaches including cost, geometric freedom, system infrastructure, robustness, and emergence to name a few. On top of this, they introduce one quantitative metric for construction efficiency, which will be utilized in this paper. By doing such, the goal is to promote the wider acceptance of such metrics in attempts to being better able to understand the application of CRC in the construction industry.

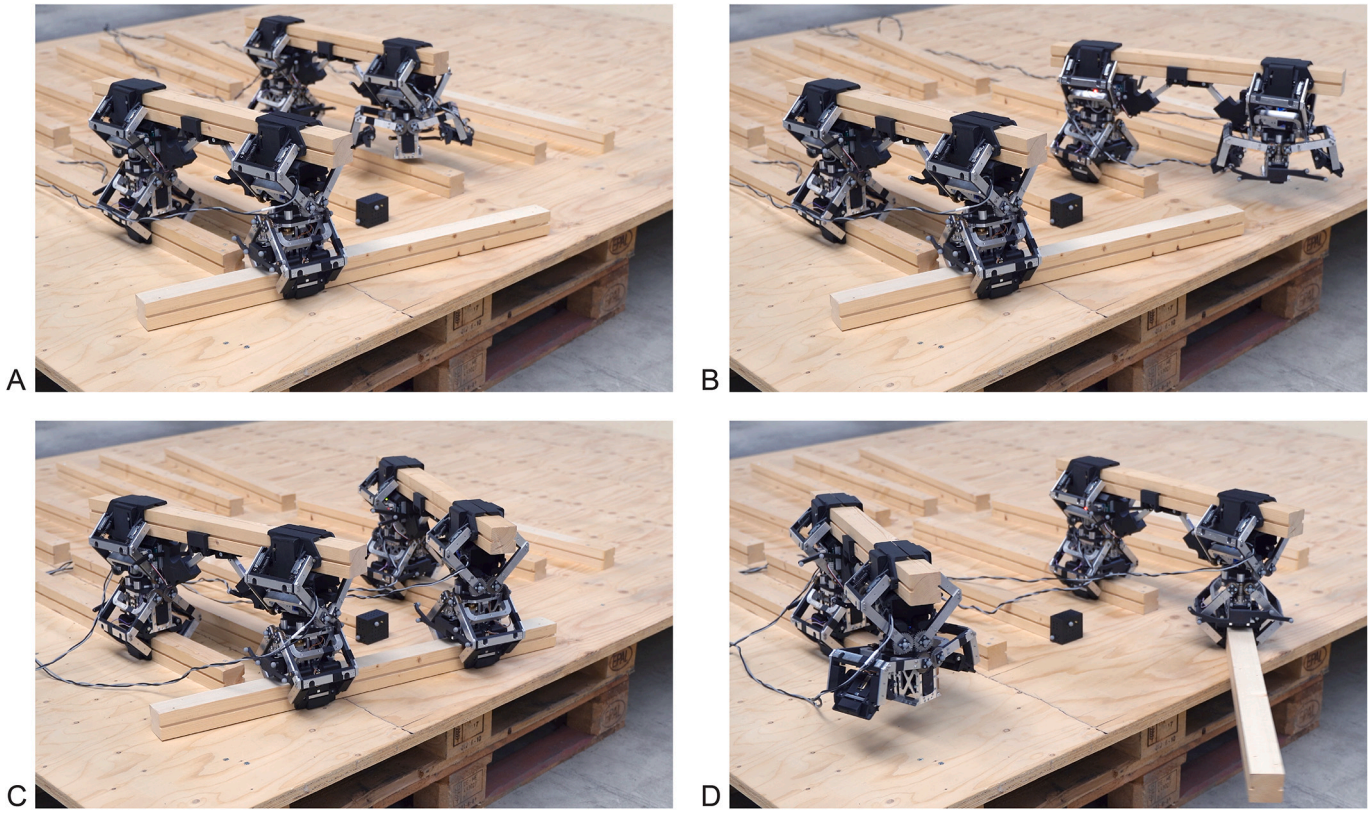


Fig. 4. Image sequence from the assembly of a large-scale in-plane timber structure, which requires two kinematic chains to collaborate (A-D). The kinematic chain in the front left holds a timber strut and waits for another kinematic chain to locomote to it (A-B). Another kinematic chain comes and picks up the timber strut and rotates it around the exterior of the already bult structure in the direction of where it will be placed in the structure (C-D).

3. Scope of the Research & Organization of the paper

This research builds upon a modular CRC system for timber construction [12]. The system is composed of two major elements: robotic actuators and timber struts. As the robotic actuators cannot locomote on their own, they must leverage the timber struts in order to move and perform assembly tasks in a shared workspace. This is achieved by identical robotic actuators gripping and releasing timber struts to form modular assemblies called kinematic chains of various combinations of the two elements of the system. Through the collaboration of multiple kinematic chains, timber struts can be moved around and in turn be assembled into structures. Two kinematic chains with two robotic actuators, the kinematics of which are described in Fig. 3, is the minimum requirement to assemble timber struts. A series of physical demonstrations using kinematic chains of such complexity have proven the ability of the system to preform construction tasks, including the locomotion of robotic actuators and timber struts, the dynamic rearrangement of kinematic chains, and the transport of a timber strut for assembly [12]. Each construction task, however, only require a few actions, rotation, and gripping, from the robotic actuators involved in the task.

The next step for validating the CRC system was to prove the ability of the system to function at longer horizon problems. Therefore, this paper builds upon the construction task demonstrated previously [12], through the assembly of an in-plane architectural timber structure using two kinematic chains, each equipped with two robotic actuators. The kinematic chains perform an iterative process of locomotion and transportation to do this (Fig. 4). This meant the (i) execution of robotic actions with numerous timber struts, which when produced at scale have a range of machining tolerances, and (ii) the fixation of timber struts with material connections, which reflect the challenges of material tolerances and material connections experienced in CRC. To deal with both problems and in turn increase the robustness of the system, updates to the physical CRC system were required.

In order to address this further development, this paper is organized into the following sections. **Section 4** presents the co-design of the robotic actuator hardware to the timber strut building material to deal with material tolerances and a characterization of the performance of gripping of the robotic actuator in greater detail. **Section 5** introduces a connection mechanism for assembling timber struts and further reports on testing of the mechanism. The updated robotic actuator with the connection mechanism is depicted in Fig. 5. With these two updates, the robotic actuator electronics and control is explained in **Section 6**. A large-scale in-plane timber building prototype is then discussed in **Section 7**.

Section 8 addresses the goal of this paper related to the evaluation of the CRC system. It presents an in-depth evaluation of the proposed CRC system based on various performance metrics utilizing the prototype built for this paper and compares it to other robotic construction systems for timber as well as CRC systems that use other materials. **Section 9** concludes the paper with final remarks.

4. Development of the robotic system for material tolerance

Within the proposed modular CRC system, the main active element is the robotic actuator [12]. Each robotic actuator contains a single motor-driven rotational axis. This rotational axis separates the robotic actuator into two halves, each half is equipped with a gripper. The grippers face in opposing directions. The robotic actuator can open and close the grippers around passive timber struts of dimension 50 mm by 50 mm (i) to form kinematic chains for locomotion and (ii) to lift and transport the timber struts in the system for assembly. The timber struts contain a groove along their length which matches the tongue geometry of the robotic actuator's grippers to increase the surface area for more stable connections between timber struts and robotic actuators. Each half of the robotic actuator contains additional components beyond those required for gripping. The mechanisms for rotation are housed in the lower gripper, while the upper gripper contains the essential electronics for communication and control including the microcontroller and Bluetooth module. The upper gripper also holds the battery.

In attempting to assemble a timber building prototype (Fig. 1) using robotic actuators composed into kinematic chains with two robotic actuators and one strut, the kinematic chains occasionally failed to stably grip some of the milled timber struts. Failed grips results in kinematic chains tilting from vertical in the direction of the cantilever (Fig. 6). When too large tilting occurs, kinematic chains can no longer perform construction tasks, neither locomotion nor transportation, as when they rotate the hanging robotic actuator would collide with the layer of timber struts they are building in. Small angles of tilting however be accounted for by the hardware, meaning the gripping would still be considered successful. The allowable tilting angle ($\theta_{t,\ allowable}$) for successful gripping depends on the distance between the robotic actuators

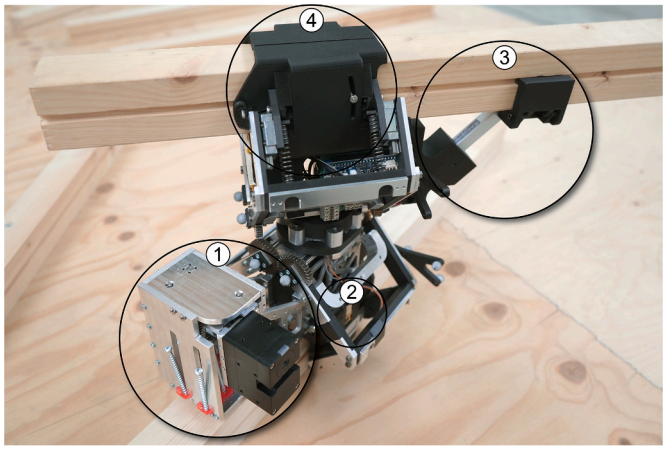


Fig. 5. Photograph of the robotic actuator with updates to adjust for material connections (1) and material tolerances (2–4). The updates are labelled with circles. A custom screwdriving effector is connected to the bottom half of the robotic actuator (1), the tongue and groove mechanism of the lower gripper is now motorized to increase contact forces (2) and a mechanism for adjusting the tilt of a kinematic chain is assembled to the upper half of the robotic actuator (3), which also affects the design of the upper gripper (4).

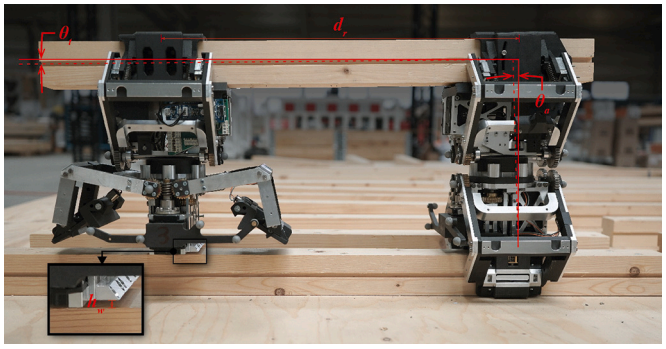


Fig. 6. Tilting from the robotic actuator of the kinematic chain that is gripping on the plane of timber struts which it locomotes and builds. Tilting occurs from the robotic actuator that is gripping in the direction of the cantilever (θ_a) and in turn tilting of the entire kinematic chain (θ_t). The red solid line indicates the vertical and horizontal lines of where the kinematic chains should be, and the red dashed lines are the locations of the kinematic chains in the real world. Calculation of allowable tilting angle that permit the kinematic chains to function is based on two measurement marked in the image: the distance between the robotic actuators (d_r) and the height between the bottom of the hanging robotic actuator and surface of the timber strut in the kinematic chain (h_w). (For interpretation of the references to colour in this figure legend, the reader is referred to the web version of this article.)

(d_r) and height between the bottom of the hanging robotic actuator and surface of the timber strut in the kinematic chain (h_w). When h_w is 7.7 *mm,* the hanging robotic actuator in a kinematic chain can grip the timber strut below it. $\theta_{t,\ allowable}$ can be calculated as follows:

$$\theta_{t,allowable} = sin\left(\frac{h_w}{d_r}\right) \quad (1)$$

Large tilting errors could not be overcome with the two previously codesigned passive mechanisms in the gripper of the robotic actuator and timber strut, which aimed at stiffening the body of the robotic actuator relative to the timber strut it is grip [12]. After analysis of the potential sources of the problem, it was identified that material tolerances in the machining of the timber struts was the main factor in causing such failed grips. Due to the small number of timber struts utilized in the initial construction task demonstrations [12], the milling tolerances of the timber struts was negligible. However, in the assembly of large quantities of timber struts, the managing of milling tolerances is a challenge. When 50 struts were manually machined for the prototype, errors in the milling of the groove of the timber struts accumulated in different ways (Fig. 7). The errors measured in the grooves of the 50 timber struts were the oversizing of grooves by a range from 0 to 1.4 mm and the shifting of the grooves up or down relative to the center of the timber strut by a range of 0 to 1.0 mm.

Each of the machining errors, the range of which are explained in Fig. 7, cause the robotic actuator that holds the weight of a kinematic chain to tilt, and in extreme cases stop the other actuator from gripping any further timber struts. As the interaction between the robotic actuator and timber struts is the basis for success of any construction task, further co-design of robotic actuator was conducted to deal with the issues of material tolerances in the timber struts. The main objective is to allow for the robotic actuators to deal with the tolerances in the machining of the groove in the timber strut.

4.1. Updates to the previous gripper mechanisms

The first update to the robotic actuator was to the two original passive mechanisms integrated into the robotic actuator: (i) the tongue and groove between the robotic actuator and timber strut, and (ii) the clipping mechanism on the gripper paddle (Fig. 8).

The tongue and groove connection previously relied on perfectly matching geometrical conditions in which the tongue of the gripper paddle fit precisely into the groove milled into the timber strut.

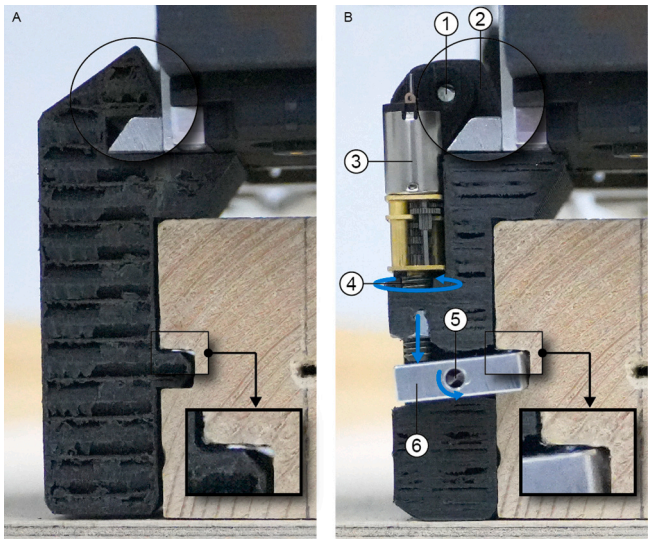


Fig. 8. Previous (A) and updated (B) designs of the gripper mechanisms of the robotic actuator. The gripper paddle was cut in half to display the inside of the mechanisms. The circled regions highlight the updated clipping mechanism and the boxes highlight the new alignment mechanism. Zoomed in images of the tongue and groove are shown to visualize the contact or lack thereof in each scenario. The blue arrows denote motions related to actuation of the tongue mechanism in the updated design (B). The numbered parts in the diagram highlight the new parts of mechanism. The parts are as follows: axis of rotation for the new clipping mechanism (1), custom rotating clip (2), DC motor for tongue mechanism (3), lead screw (4), axis of rotation of metal tongue (5) and metal tongue (6). (For interpretation of the references to colour in this figure legend, the reader is referred to the web version of this article.)

However, with tolerances in the machining of the timber, it is not possible to assume such conditions. This resulted in the tongue of the gripper not filling the space of the groove (Fig. 8A). Specifically, when the tongue does not make contact with the top of the groove, large tilting angles are observed. Therefore, the tongue on the gripper of the robotic actuator was modified to allow for errors in the milling of the groove (Fig. 8B). First, the tongue is now made from metal and smaller in height than the groove. This helps to align and fit into the groove when the robotic actuator is closing the gripper arms. Second, the tongue is actuated by a small, geared DC motor after the gripper is closed around

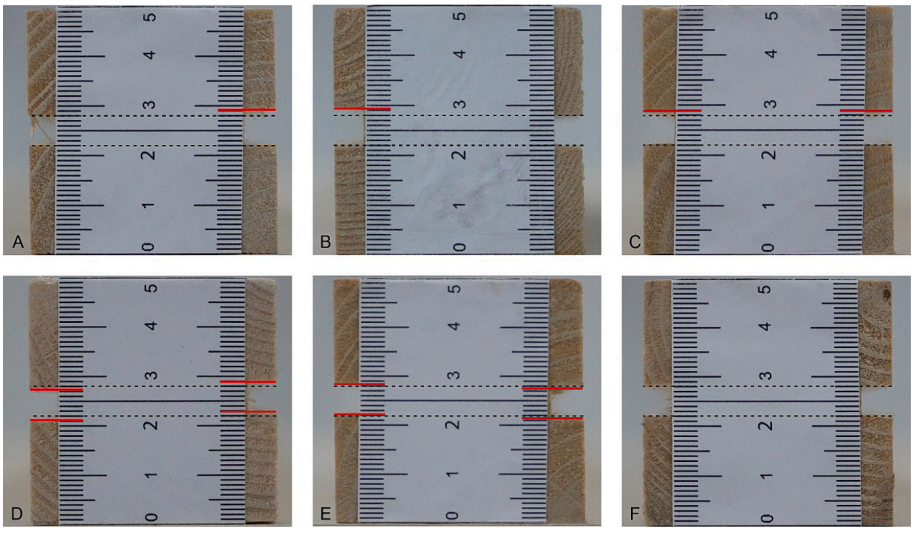


Fig. 7. Material machining tolerances commonly found in the milling of the grooves in the timber struts: Single oversized groove on one side (A-B), both grooves oversized (C), shifted grooves (D-E) and precisely milled (F). The black dashed lines indicate where a precisely milled groove should align, and the red lines indicate the placement of the groove after milling. (For interpretation of the references to colour in this figure legend, the reader is referred to the web version of this article.)

the timber strut to ensure contact between the tongue and groove on the strut.

The clipping mechanism rigidizes the gripper paddle and robotic body together and was also adjusted. The previous design relied on the matching of exact geometry, in which one geometry from the robot body slides into the geometry of the gripper paddle (Fig. 8A). This is problematic when considering misalignments caused from irregularities in the machining of the timber struts as small tolerances cause friction in the mechanism. Large amounts of friction prevent the matching interlocking of the geometries to take into effect and thus the mechanism fails, providing no additional benefit in rigidizing the robotic actuator relative to timber struts. For the clipping mechanism to function, the clip on the gripper paddle was augmented with the ability to rotate, guaranteeing that it encases the matching geometry on the side of the body of the robotic actuator (Fig. 9).

4.2. Gripper performance test and design verification

Experiments were conducted to characterize the performance of these updates to the bottom gripper of the robotic actuator. The previous gripper design as well as the updated gripper design were assessed by rotating a kinematic chain (θ_r) and measuring the tilting of the kinematic chain from the top of the robotic actuator that holds the kinematic chain (θ_t). This was conducted on timber struts with different tolerances in the milled groove and at different distances of the robotic actuators in the kinematic chain (d_r). This included a timber strut in which the groove on one side of the strut was oversized, the grooves were oversized on both sizes and the grooves shifted from the center of the strut as depicted in Fig. 7. For timber struts with a single oversized groove and shifted grooves, the experiment was conducted twice on struts showing similar errors but on different sides of the timber strut. Both the previous and updated gripper were tested against a precisely machined groove as a base for comparison. The distances between robotic actuator tested were 40 cm, 45 cm, and 50 cm. Using **Eq. 1**, the maximum allowable tilting angles are 1.1°, 0.98°, and 0.88° respectively.

Fig. 10 compares the tilting angles (θ_t) between the previous and updated gripper designs according to the different rotating angles (θ_r) of the kinematic chain relative to the strut that it is gripping and robotic actuator distances (d_r). Rotating angles (θ_r) around 90° and 270° cause the maximum tilting due to the directional characteristic of the applied torque from the hanged robot, which is working in direct opposition to the gripper holding the kinematic chain. Longer distances between the

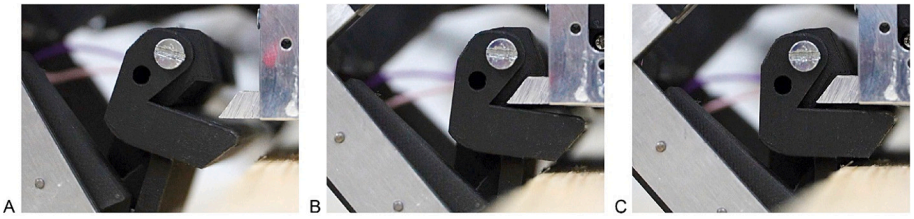


Fig. 9. Sequence of images showcasing the functionality of the updated clipping mechanism (A-C). Rotation of the clip on the gripper paddle occurs through contact with the body of the robotic actuator.

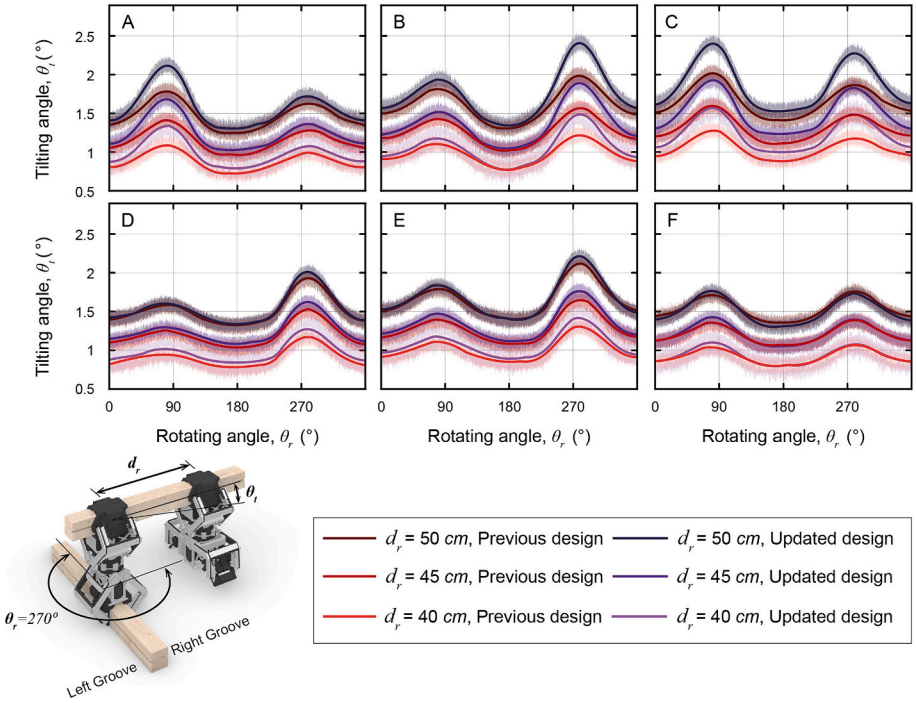


Fig. 10. Performance evaluation for the previous and updated gripper design. Comparison of measured tilting angle of the kinematic chain (θ_t) according to different distances between robotic actuators in the kinematic chain (d_r) and different angles of the actuators in the kinematic chain relative to the strut that it is gripping (θ_r). The graphic in the bottom left explains the test setup, indicating how each of the variables are measured. Each graph indicates 10 trails conducted on timber struts with the following milling tolerance: Oversized right groove (A), oversized left groove (B), both grooves oversized (C), left groove shift down and right groove shifted up (D), left groove shifted up and right groove shifted down (E) and precisely milled (F). The range of collected data from the trails is shown via the transparent regions of each colour.

robotic actuators cause larger tilting angles due to the larger cantilever that the kinematic chain must support.

The updated gripper reduces the tilting of the kinematic chain in all cases. Table 1 and Fig. 11 shows improved ratios of the tilting angles from the updated gripper design. The ratio is defined by dividing the maximum tilting angle of the updated gripper design with the tilting angle at the same rotating angle of the old gripper design. The experiments confirm that when the groove is oversized or higher on the opposite side of which the kinematic chain cantilevers, tilting is the greatest. In the case when the groove is precisely milled or shifted down on the same side of the cantilever, the performance is similar to the precisely milled groove with the updated gripper (Fig. 10F).

Specifically, the tilting angles from one or both oversized grooves (Fig. 10A-C) preform similarly to the precisely machined grooves (Fig. 10F). However, the improvements are not enough for distances greater than 40 cm between the robots as the tilting angle exceeds the allowable tilting angle. Although the updates to the gripper do also improve tilting in cases with shifted grooves (Fig. 10D and (Fig. 10E), the titling that such grooves cause is still too large to reach the allowable tilting angle in all rotating angles. This means that the kinematic chain collides with the layer of timber struts they are building upon.

4.3. Additional tilting adjustment mechanism

Although the updates improved the performance of the gripper, there were still certain scenarios at which the kinematic chain tilted more than $\theta_{t,\ allowable}$, with the most extreme case of with 50 cm between the two robotic actuators having a tilting angle of 2.12° and only 0.88° is allowable. Furthermore, there was also variance experienced in the performance even with similar milling errors, as seen by comparing two oversized groove cases (Fig. 11A and Fig. 11B) as well as two different shifted groove cases (Fig. 11D and Fig. 11E).

As a result, an additional mechanism was integrated into the robotic actuator that would allow for adjustment of any tilting above that allowable of the kinematic chain from the robotic actuator that holds it (Fig. 13). A linear actuator was integrated that spans between the upper body of the robotic actuator and the timber strut. When designing the new mechanism two forces must be considered in the selection of a suitable linear actuator: the necessary lifting force and the permissible side load on the linear actuator. Fig. 12A includes a schematic kinematic diagram which highlights the applied loads to the linear actuator. The necessary lifting force and applied side load can be calculated as follows:

$$\begin{aligned}
\vec{P}_{mr} &= \left(0.5d_r + d_p\right)e^{(\pi+\theta_p)i} + d_{cm}e^{\left(-\frac{\pi}{2}+\theta_p\right)i} \\
\vec{P}_{mt} &= d_p e^{(\pi+\theta_p)i},\ \vec{P}_l = d_l e^{(\pi+\theta_p)i} \\
F_l &= \frac{\left(\left|Re\left(\vec{P}_{mr}\right)\right| m_r g + \left|Re\left(\vec{P}_{mt}\right)\right| m_t g\right)}{\left(cos(\theta_l)cos(\theta_p)\left|Re\left(\vec{P}_l\right)\right|\right)} \\
F_s &= (m_r + m_t)gsin(\theta_l)
\end{aligned} \tag{2}$$

where $\vec{P}_{mr}$, $\vec{P}_{mt}$ and $\vec{P}_l$ are vectors between the pivot point of the new mechanism and mass centers and the contact point of the linear actuator on the timber strut, i is the imaginary unit, F_l is the minimum force required to lift up the kinematic chain, F_s is the side load to the linear actuator, $Re\left(\vec{P}\right)$ outputs real parts of the vector $\vec{P}$, m_r is the mass of

Table 1
Performance evaluation of the tilting angle of the kinematic chain for the previous and updated gripper designs. The numbers were averaged from 10 trials. The improvement is calculated using the maximum point in the averaged tilting angles with the updated gripper and the maximum point in the averaged tilting angles with previous gripper. The improvement includes the average improvement as well as the bounds for the maximum and minimum improvements during 10 trials. The cases refer to Fig. 7.

Case	d_r (mm)	Previous (°)	Updated (°)	Improvement (%)	Case	d_r (mm)	Previous (°)	Updated (°)	Improvement (%)
Oversized right (A)	40	1.35	1.09	18.7 (+1.9, −1.94)	Oversized left (B)	40	1.49	1.22	17.95 (+2.63,-2.93)
	45	1.69	1.42	16.44 (+1.8, −2)		45	1.9	1.57	17.07 (+2.01, −1.29)
	50	2.12	1.79	15.79 (+2.3, −1.62)		50	2.41	1.99	17.23 (+2.52, −1.83)
Oversized both (C)	40	1.5	1.19	20.9 (+3, −3.1)	Left down, right up (D)	40	1.27	1.17	8.09 (+3.11, −3.41)
	45	1.83	1.49	18.92 (+2.4, −2.16)		45	1.63	1.52	6.24 (+2.08, −2.75)
	50	2.28	1.87	17.85 (+1.3,-1.93)		50	2.01	1.94	3.81 (+1.94, −1.24)
Left up, right down (E)	40	1.42	1.31	7.81 (+2.4, −2.2)	Accurately milled (F)	40	1.1	1.03	5.58 (+3.93, −3.14)
	45	1.77	1.65	6.89 (+2.2, −2.51)		45	1.42	1.35	4.79 (+2.19, −1.94)
	50	2.22	2.12	4.54 (+1.2, −1.75)		50	1.77	1.71	2.94 (+1.27, −1.21)

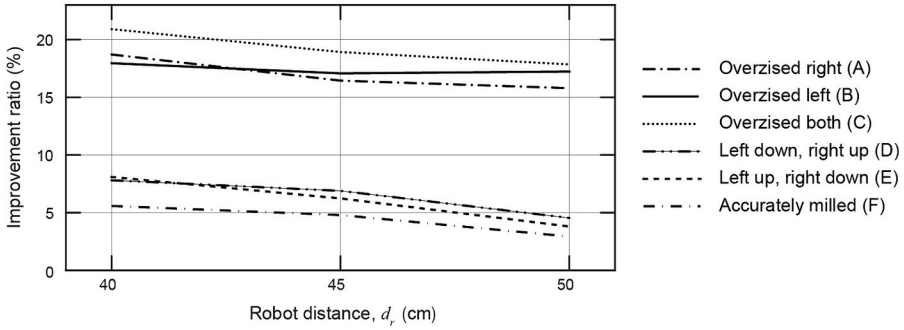


Fig. 11. Improvement ratio of tilting angle according to the robotic actuator distances (d_r) and conditions of timber strut. The improved ratio is defined as the maximum averaged tilting angle from 10 trials with the updated gripper design divided by maximum averaged tilting angle from 10 trials with the previous gripper design. The maximum tilting angles on both designs occurs when the kinematic chain is oriented perpendicular to the strut it is gripped, around 90° or 270°.

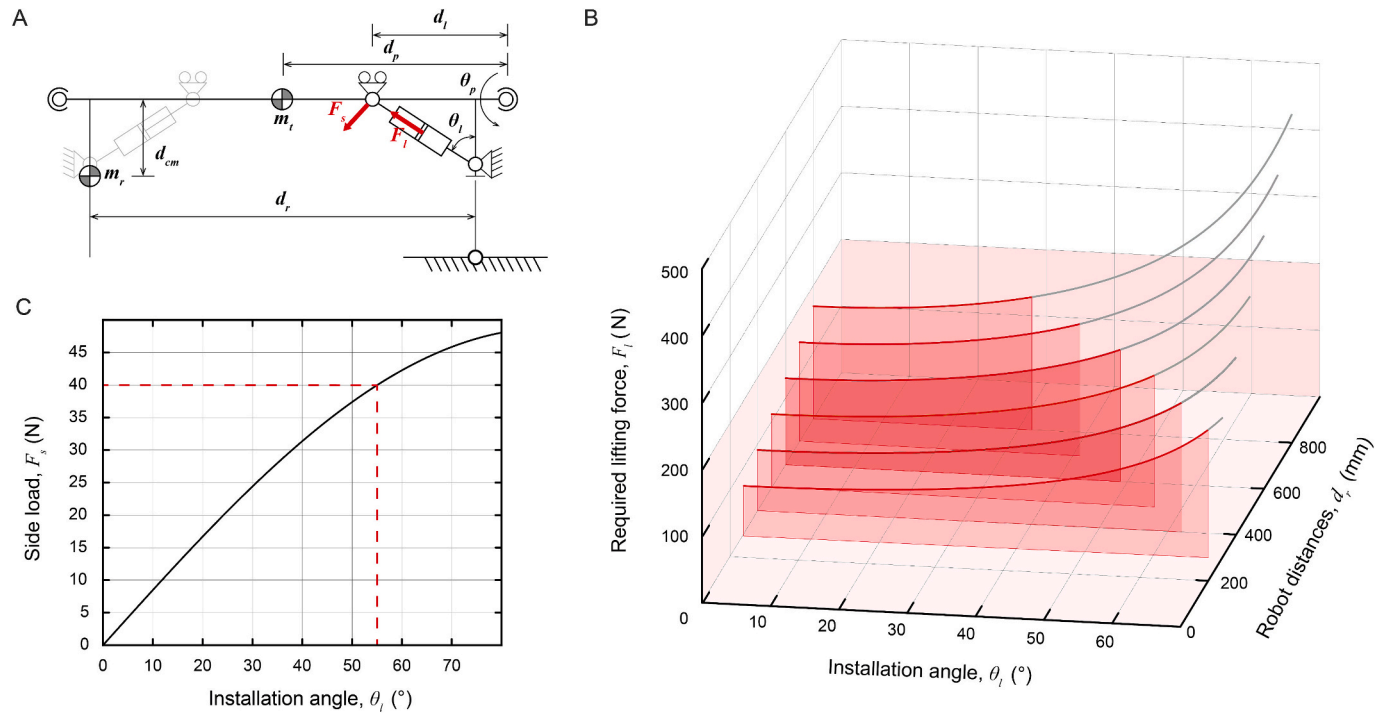


Fig. 12. Schematic kinematic diagram of kinematic chain with two robotic actuators used for calculating the forces on the lifting mechanism (A). Analysis of side load (F_s) considering the installation angle of the lifting mechanism (θ_l) (C). The red dotted lines indicates the allowable side load, 40 N, in the final design and the maximum possible installation angle, 55°, for that load. Analysis of required lifting force (F_l) considered the installation angle of the lifting mechanism (θ_l) and the distance (d_r) between the robotic actuators in the kinematic chain (B). The plotted curves represent the analysis for d_r equal to 300 mm, 400 mm, 500 mm, 600 mm, 700 mm and 800 mm. The red areas on the curves highlight the possible design options that would function given the chosen linear actuator, which has a maximum force of 200 N. (For interpretation of the references to colour in this figure legend, the reader is referred to the web version of this article.)

robotic actuator, m_t is the mass of timber strut, g is the gravitational acceleration, d_r is the distance between robotic actuator in the kinematic chain, d_p is the distance between the center of mass of the timber strut and the pivot point of the new mechanism that lifts the kinematic chain, d_l is a varying distance determined by the extension length of the linear actuator between the pivot point of the new mechanism and the contact point of the linear actuator on the timber strut, d_{cm} is the distance between the centerline of the timber strut and mass center of the robot, θ_p is the rotating angle of the kinematic chain measured from the pivot point of the mechanism and θ_l is the angle of installation of the linear actuator.

Since the adjustment of tilting occurs at angles under 3°, θ_p has minimal effect on the results of the calculation and Eq. 2 can be approximated as follows:

$$F_l = \frac{\left(m_r\left(0.5d_r + d_p\right) + m_t d_p\right)g}{\left(cos(\theta_l)d_l\right)}$$
$$F_s = (m_r + m_t)gsin(\theta_l) \quad (3)$$

The two primary parameters that affect the design of the placement of the linear actuator in the mechanism are the distance between the robotic actuators in the kinematic chain and the installation angle. Fig. 12 B-C illustrate the applied side loads and required lifting forces to the linear actuator based on the installation angles and distances between the robotic actuators in the kinematic chain.

For the final design of the mechanism, the distances between robotic actuators in a kinematic chain, d_r, was selected to be 400 *mm*., d_p and d_l were then calculated to be 265.34 *mm*, and 167.18 *mm*. Using these numbers, the minimum required lifting force and applied side load to the linear actuator are 117.2 N, and 34.8 *N*, respectively. Therefore, a linear actuator with a 200 N lifting force and 40 N allowable side load, L16 Actuonix (stroke length: 50 mm), was utilized. When actuated, the linear actuator can adjust the kinematic chain to compensate for tilt caused by errors from the act of gripping timber struts that are not perfectly milled.

Beyond compensation for tilting in the observed material tolerances (Fig. 7), this mechanism would allow for compensation that might occur from other unexpected defects in the timber strut and generally the consideration of kinematic chains with larger distances between the robotic actuators.

4.4. Robotic actuator power management

The additional actuators increase the power consumption of the robotic actuators when the grippers are in their actuated and unactuated states, therefore the calculation of the power consumption of the robotic actuator changed. Six single lithium polymer batteries (3.7 V, 2000 mAh) allow untethered power of the robotic actuator. Two battery packs, which have three serially connected batteries, are parallelly connected to achieve 11.7 V. The total capacity of the combined battery pack, $C_{b,\,\max}$, is 12 Ah. The capacity of the battery, C_b, can be calculated by subtracting the capacitance used by the electronics and their actuation in the robot as follows:

$$C_b = C_{b,max} - \sum n_m A_m t_m \quad (4)$$

where m is the type of actuation consuming current, n_m, A_m and t_m are the number of actuations, consuming current and actuation times for each actuation.

The stationary consuming current from the electronics and motors of the robotic actuator, A_s, is 0.45 A. Each individual actuation consumes additional current:

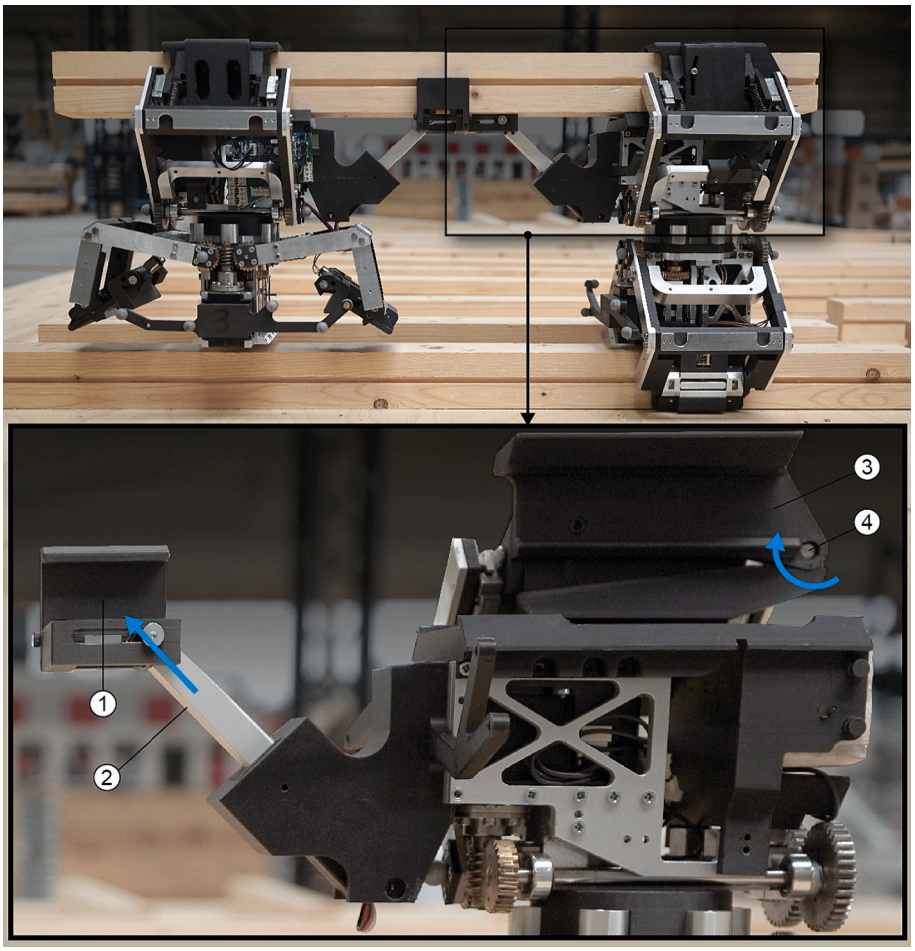


Fig. 13. Additional mechanism introduced to the robotic actuator to allow for compensation of titling in the kinematic chain. Rotation in the top gripper paddle allows for adjustment of angle caused by the linear actuator. The blue arrows in the zoomed in image on the bottom denote motions related to actuation of the mechanism. The numbered parts in the diagram highlight the parts of mechanism. The parts are as follows: custom clip with tongue for connection to timber strut (1), linear actuator (2), axis of rotation for the gripper (3), and gripper paddle (4). (For interpretation of the references to colour in this figure legend, the reader is referred to the web version of this article.)

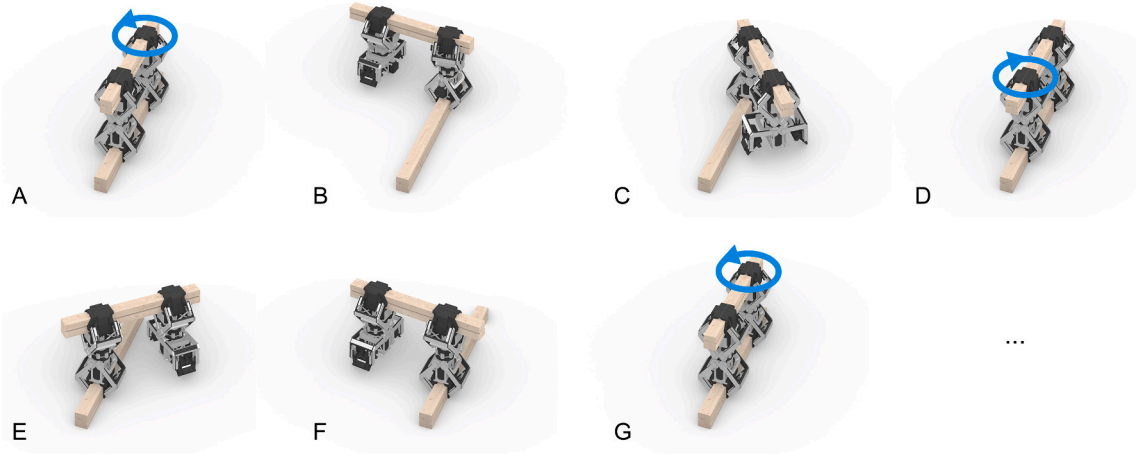


Fig. 14. First steps of locomotion sequencing utilized to estimate battery life of a single robotic actuator (A-G). One robotic actuator in the kinematic chain rotates 360° and then the other grips the strut and rotates the other 360° so that it can grip again. If the sequence is continuously repeated, a single actuator could operate for 6,8 h.

- The consuming current during rotating actuation ranges from 0.25A to 0.35 A (A_r). The range is caused by different characteristics, such as friction, of the mechanism in the physical robotic actuators.
- The current for opening or closing of the gripper is 1.4 A (A_g) and lasts 10 s (t_g) in both directions.



Fig. 15. Electronics onboard a robotic actuator: three actuators for (i) rotation, (ii) the upper gripper and (iii) the lower gripper (ROBOTIS Dynamixel MX-106), a linear actuator for tilting adjustment when assembled into a kinematic chain (Actuonix L16), two geared DC motors for the tongue actuation in the lower gripper, a microcontroller (OpenCM 9.04, ROBOTIS), a customized PCB board to integrate (i) the DC motor drivers (Pololu DRV 8833Pololu) and (ii) potentiometers to define the current limits for the DC motors of the tongue actuation (*VISHAY M43P100KB40),* and a Bluetooth module for wireless communication (BT-410 Slave, ROBOTIS).

- After gripping or before opening, the current for tongue actuation is 0.1 *A* (A_t) for 5 *s* of operation time (t_t).
- Actuation for the tilting adjustment of the kinematic chain consumes 0.25 *A* (A_a).

Considering this, Eq. 4 becomes:

$$C_b = C_{b,max} - A_s t_s - A_r t_r - n_g A_g t_g - n_t A_t t_t - A_a t_a \quad (5)$$

where t_s is the operation time after the initial power on with fully charged batteries, t_r is time for rotation, n_g is the number of times at which the gripper opens and closes, n_t is the number of tongue actuations in both directions, and t_a is elapsed time for tilting adjustment of the kinematic chain. n_s, n_r and n_a are always 1 due to continuous actuation. This equation can be used in the task and motion planning (TAMP) of a building prototype to calculate when a robotic actuator would need to be charged.

As the activity of a robotic actuator can vary, it is difficult to exactly calculate how long it can run off the battery. To give an estimation, a calculation was made considering a kinematic chain walking in place, meaning that the robotic actuators in a kinematic chain take turns rotating 360° (Fig. 14). For this, the highest current for rotation is utilized and the tilting mechanism is constantly active when holding the other robotic actuator, which is the worst-case scenario. As evident by performance testing of the robotic actuators of the updated gripper, there are only certain moments depending on the conditions of the timber strut and kinematic chain that would require the linear actuator in the tilting mechanism to be active. In this scenario, the robotic actuator can run **6,8 h** before it needs to be recharged.

4.5. Discussion of the updated robotic actuator design

The updated robotic actuator dimensions are 306.02 mm by 178.89 mm by 138.02 mm. Beyond the additional motor, linear actuator and metal tongue plate, all additional structural parts form the updates of the robotic actuator are made from micro carbon fiber filled nylon printed by a Markforged Onyx Pro (Gen 2) 3D printer. The combination of the new parts made the new weight of the robotic actuator 3.3 kg. A custom printed circuit board (PCB) board was also developed to integrate the electronic components for command processing, actuator control, wireless communication, sensing, and power management (Fig. 15).

Table 2 outlines the enhancements achieved with the updated gripper mechanism across all angles of rotation. Although the updated gripper mechanisms reduces tilting in kinematic chains, particularly in cases involving oversized grooves, it doesn't eliminate all tilting problems as the robot distance increases and grooves shift on either side of the timber strut. For kinematic chains with 40 cm between the robotic actuators, 86.1% of angles in the full 360° of rotation can be achieved without failure in the gripping across all types of machining errors in the groove of the timber strut.

To adjust for the remaining angles and allow for larger distances between robotic actuators in kinematic chains, a mechanism to adjust for tilt was incorporated into the design of the robotic actuator. This mechanism is capable of correcting tilting by 5°, which can compensate for the enlarged or shifted grooves encountered with the kinematic chains distances tested.

The equation used to design the new mechanism for tilting adjustment, **Eq. 2**, represents a static analysis. It does not account for the dynamic effects of the new mechanism, which can impact the performance of the robotic actuators. In terms of rotation of the robotic actuator around their main axis, the direction of the dynamic load from the new mechanism does not align with the rotating direction; thus, the new mechanism does not affect the rotation of a robotic actuator. The dynamics of the new mechanism can, however, influence the gripping stability of the robotic actuator, as its motion imposes an additional load on the gripper. Nevertheless, no gripping failures were observed during the assembly of the large-scale prototype discussed in **Section 7**, and thus the dynamics of the new mechanism were proven to be manageable by the mechatronic design of the robotic actuator.

These additional developments of the robotic actuator highlight how enhanced co-design of the system can address material tolerances in CRC, allowing for the compensation of machining errors in the building material. This contributes to the larger context of dealing with error in CRC, which currently focuses on algorithmic approaches for error mitigation and correction in the sequential buildup of structures [14] [27,28]. With further advances in both hardware techniques and control software, CRC systems can become more robust for the assembly of real architectural structures.

5. Development of a lightweight Mobile timber connection mechanism

The other important development of the proposed CRC system for the assembly of a large-scale in-plane timber building prototype was the development of an effector that enables the fixation of the timber struts. The effector addresses the problem of material connections commonly found in CRC by introducing hardware that enables robotic actuators to connect the timber struts within the structure.

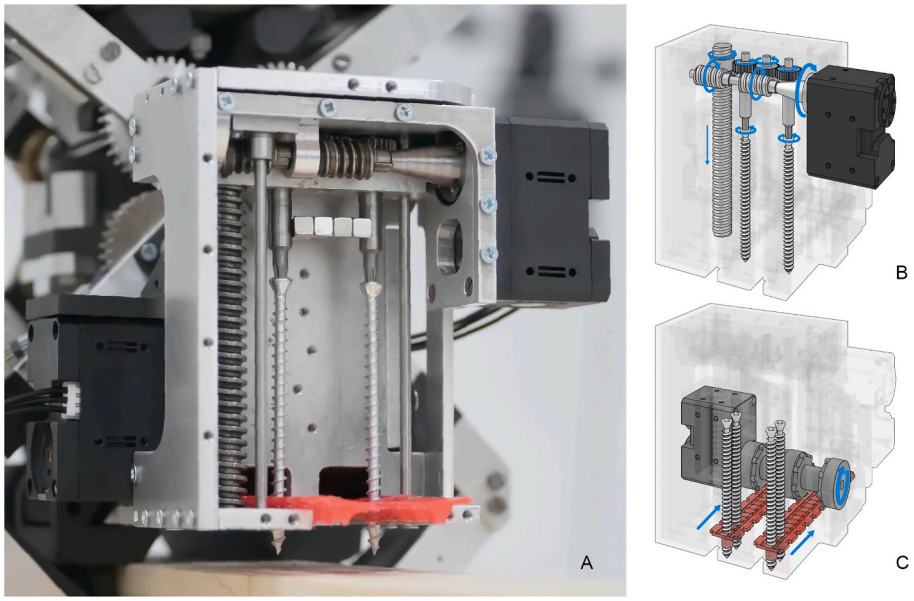


Fig. 16. Screwdriving effector developed for the CRC system (A). The effector contains two motors which perform the two functions of the drill: screwdriving and screw feeding. The motor for screwdriving is connected to a gear box which rotates the screw bits and simultaneously drives them in the direction of the timber (B). The second motor for screw feeding is connected to a 3D printed drum which locks into a plastic belt of screws (C). Rotation of the drum feeds new screws in the direction of the screw bits once a connection is complete. The blue arrows denote motions related to actuation of the mechanism. (For interpretation of the references to colour in this figure legend, the reader is referred to the web version of this article.)

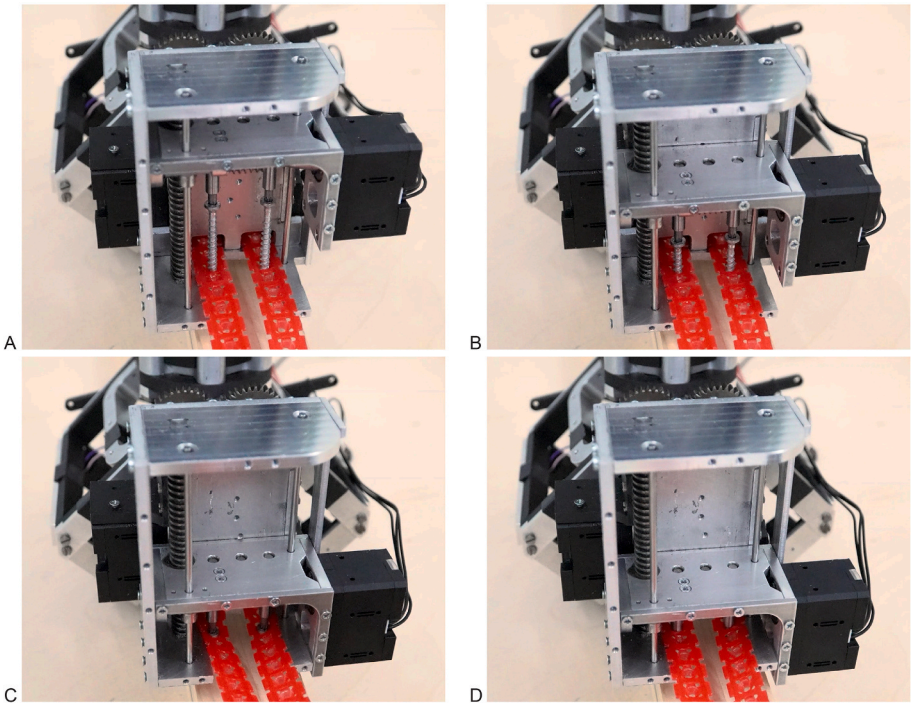


Fig. 17. Image sequence from the screwdriving effector (A-D).

5.1. Selection criteria

There were three significant criteria for the selection of a connection strategy before the development of the hardware for it. The first was to utilize a connection strategy that is already existing in timber construction. Considering the long-standing history of timber construction and resulting catalogue of connection types, investigation was limited to already existing connection strategies in timber construction. The second major factor was the force required to achieve the connection, considering the small scale and low strength of the robotic actuator. The aim is to equip the robotic actuator with the hardware to perform the connection on in own. The last criterion was that, once a timber strut is fixed, the connection should allow for the potential for it to be disassembled. This criterion was stipulated because one of the potentials of CRC systems is that the robotic actuators can functionally adapt a structure throughout the construction or operation phases of it. The connection needs to be reversible to allow for this.

Using these defined criteria, screwed connections were selected for

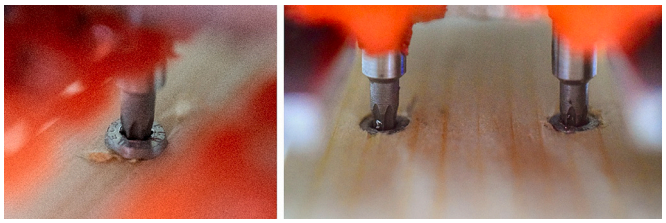


Fig. 18. Close up image of just before completed and of completed screwdriving. The orange in the images are the plastic belts which hold the screws.

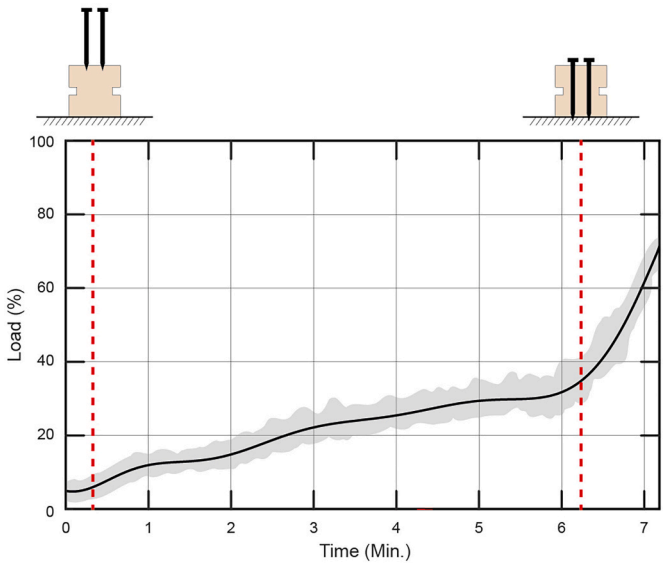


Fig. 19. Screwdriving effector average load consumption. Load is measured in percentage of the total load of the motor, *ROBOTIS* XC430-W240 (stall torque of 1.9 N.m at 12v and 1.4 A), that drives the screwdriving during the completion of a screw connection. The grey area represents the range of load consumption as tested on 3 spruce timber struts at three different locations along the length of the strut. The spikes in the graph occur at specific moments in the screwdriving process. They are indicated by the icons above the dashed red lines: when the screw enters the strut (left) and when the screw exits the strut and enters the timber beneath it (right). (For interpretation of the references to colour in this figure legend, the reader is referred to the web version of this article.)

further development. Table 3 details the selection criteria of other types of timber connection methods that are not satisfied. Craftsman-type connections were ruled out due to the high contact forces that come from slight misalignment and therefore accuracy required for their assembly [48]. There are various research projects that are currently investigating how to deal with this problem, include that from Leung et al. [44], Apolinarska et al. [48] and Kramberger et al. [49]. Doweled connections face similar challenges. Although other research is similarly investigating how to make dowels for robotic fabrication [50,51], they were not chosen for this research in order to avoid high friction that often has to be overcome with the insertion of dowels. Bolted connections were excluded not due to the criteria above but due to the current building system capable of being achieved by the CRC system. With bolt connections, both sides of the connection must be accessed which is not possible with the in-plane structures being built.

5.2. Screwdriving effector design

The effector to enable a robotic actuator with the ability to perform screwed connections also needed to satisfy a series of design criteria. The first design criteria is that the screwdriving effector should be a maximum of half the height of the robotic actuator. It can only span between the timber strut that it will screw and the slewing ring from which the robotic actuator rotates. Otherwise, the robotic actuator is not able to rotate, removing the main functionality which allows it to form kinematic chains for locomotion and assembly of timber struts. The second design criteria for the screwdriving effector is that it should make rigid connections. The insertion of a single screw at one point along the length of a timber strut would potentially allow for rotation around that point. To avoid this, the robotic should insert two screws when inserting the connection. Third, the effector should allow the robotic actuator to perform multiple connections in series. The reason behind this criterion is that a timber strut can therefore be connected in more than one point when assembled into the structure. This means that a screwing effector must be able to hold more than just a single set of screws. Finally, the effector should be as compact, simple, and lightweight as possible, criteria which are carried over from the general design intension for the entire CRC system. This includes the integration of as few electronic actuators as possible.

To meet these criterion, a screwdriving effector was design and prototyped with a final dimension of 109.83 mm by 118.5 mm by 123.5 mm (Fig. 16A). The mechanism of the effector was derived based on an auto-feed screwdriver, which is often used in drywall construction. An initial sketch for the effector was presented in Leder et al. [52]. However due to the changes in the robotic actuator hardware, a new effector needed to be developed, especially considering the first design criteria of fitting on half of the robotic actuator. A full explanation of the mechanism of the effector are presented in this section.

The effector contains two continuous rotation servomotors, which perform the two major functions: (i) inserting the screws and (ii) feeding the new screws for the next connection. The functionality of the drill is shown in the image sequence in Fig. 17. When the first motor is actuated, its force is translated for the rotation of the drill bits as well as for the driving of the drill bits in the direction of the connection (Fig. 16B). This is done by augmenting the motor with a custom gear box. The actuation of the first motor is transferred to two sets of gears through a 20:1 worm gear connection. One set of gears in the gear box controls the movement in the direction of the connection using a trapezoidal shaft and nut, and the other set is used to rotate the drill bits using spur gears. An important consideration for the mechanism is to maintain the same speed of travel of the screw bits in the direction of the connection with the amount the screw is inserted into the timber struts. To do this, the pitch of the threads of the screws (3 mm) was matched to the pitch of the trapezoidal shaft.

The second motor controls a plastic belt of screws, which allows it to feed screws to the drill bits (Fig. 16C). After a connection is completed meaning two screws are simultaneously inserted (Fig. 18), the drill bits must first travel back to the top of the effector through the reverse rotation of the first motor. After this, the second motor can rotate to advance the screws in the plastic belt. Magnets that surround the drill bit orient the screws to the drill bit so that the two align when drilling of the screws begin.

5.3. Screwdriving performance test, design verification and power management

To analyze its performance, the screwdriving effector was tested on a series of spruce struts, a common timber building material and the material utilized with the CRC system, with 60 mm screws. As the properties of timber can change along their cross section due to knots or other defects in the wood, the effector was tested on three different struts at three different locations. The aim of this was to test the functionality of the effector but to also measure the load when screwing and therefore be able to update the formula for the power consumption of the robotic actuator. During each of the nine tests, the load of the motor performing the drilling was recorded. A video from these tests can be found in **Supplementary Media S1-S2.**

Fig. 19 is a summary of the results of these tests, displaying the percentage of total load on the motor, *ROBOTIS* XC430-W240, that is driving the screws during the completion of a connection. The load is measured directly from the motor, which has a maximum stall torque of 1.9 N.m. There are two spikes in the graph that indicate crucial moments in the screw driving process. The first spike is when the screws begin to penetrate the timber strut. As the screws continue to penetrate the struts, the contact surface between the screws and strut increases; therefore, the load increases as well. The second spike occurs when the screw exits the timber strut and enters the timber beneath it. This drastically increases the load on the screwdriving effector. However, the load in all tests were under the maximum of the motor which actuates the screwdriving in the effector.

Using these results, Eq. 5 is updated in the following manner:

$$C_b = C_{b,max} - A_s t_e - A_r t_r - n_g A_g t_g - n_t A_t t_t - A_a t_a - n_f A_f t_f - n_d A_d t_d \quad (6)$$

where the additional variables are n_f for the number of feeding actuation, A_f for the current while screw feeding, t_f for the time of screw feeding, n_d for the number of times screwdriving occurs, A_d for the current while screwdriving and t_d for the time of screwdriving. Screw feeding has a duration of 10 s (t_f) and consumes 0.05 A of current (A_f). The current consumed while screwdriving changes over time as evident by Fig. 19. The battery consumption per occurrence of screwdriving is 0.04 Ah.

5.4. Summary and discussion of effector

The structural parts of the screwdriving effector were milled from aluminum. The effector weighs 0.88 kg, meaning the total weight of the robotic actuator with the effector is 4.18 kg. Control of the actuators is conducted through the main PCB board of the robotic actuator.

While conducting the performance test, it was discovered that the

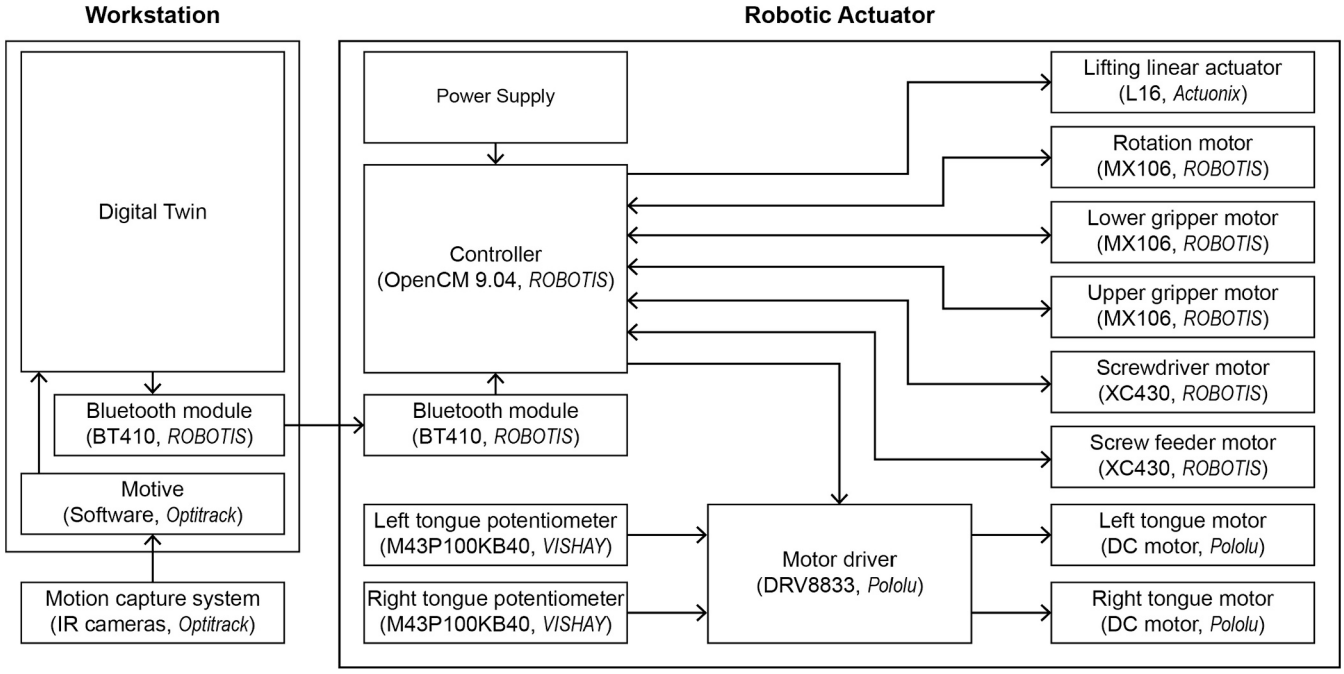


Fig. 20. Block diagram of the electronic control system, showing relationships to a workstation and single robotic actuator. The robotic actuator has an onboard controller, ROBOTIS OpenCM 9.04, with three UART communicatio ports, Bluetooth compatibility, a USB port, and several PWM ports. The UART communications support TTL (Transistor-Transistor-Logic) communication for interfacing with ROBOTIS servo motors, Bluetooth communication with the ROBOTIS BT410 to the workstation and USB communication for code uploading and debugging. The PWM ports on the controller generate signals for the motor drivers, Pololu DRV8833, and the linear actuator. The motor driver incorporates dual H-bridge drivers designed to operate brushed DC motors for the tongue actuation, providing a current of 1.2 A for each channel. Furthermore, the motor driver has current limiting for each channel, which can be set using a potentiometer.

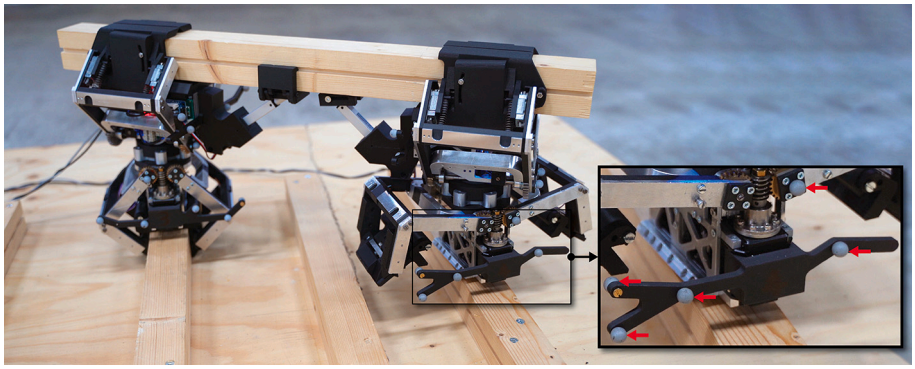


Fig. 21. Photograph of kinematic chain to show reflective markers utilized to track the robotic actuators with the external motion capture system. The markers are pointed at with red arrows in the zoomed image. (For interpretation of the references to colour in this figure legend, the reader is referred to the web version of this article.)

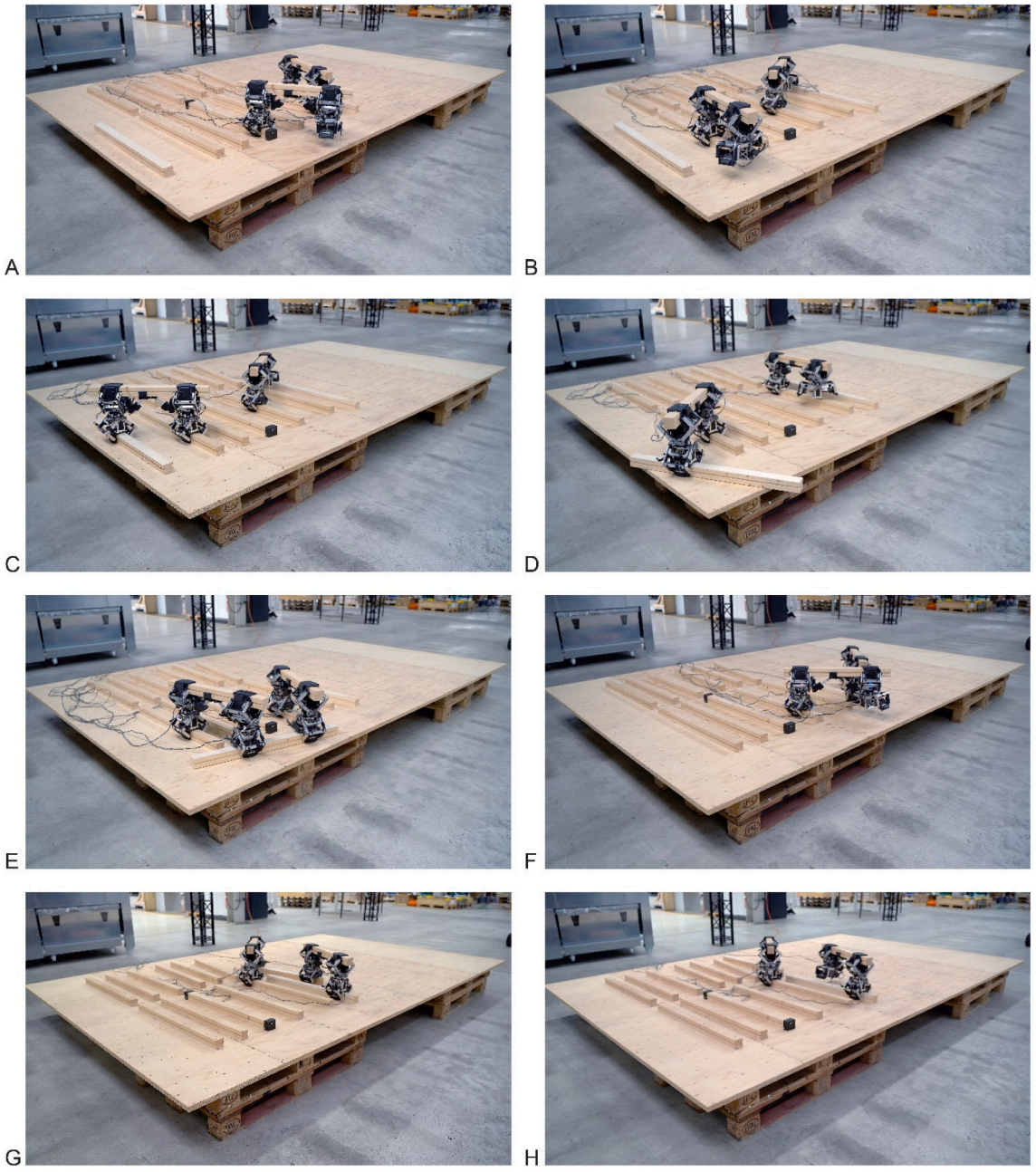


Fig. 22. Image sequence from the assembly of the larger scale prototype made at the Instrumentation Platform for Distributed Robotics at the IntCDC's Large Scale Construction Robotics Laboratory (A-H). The images show the process of assembling a single timber strut. The left most timber strut in (A) shows were timber struts are fed into the system for assembly.

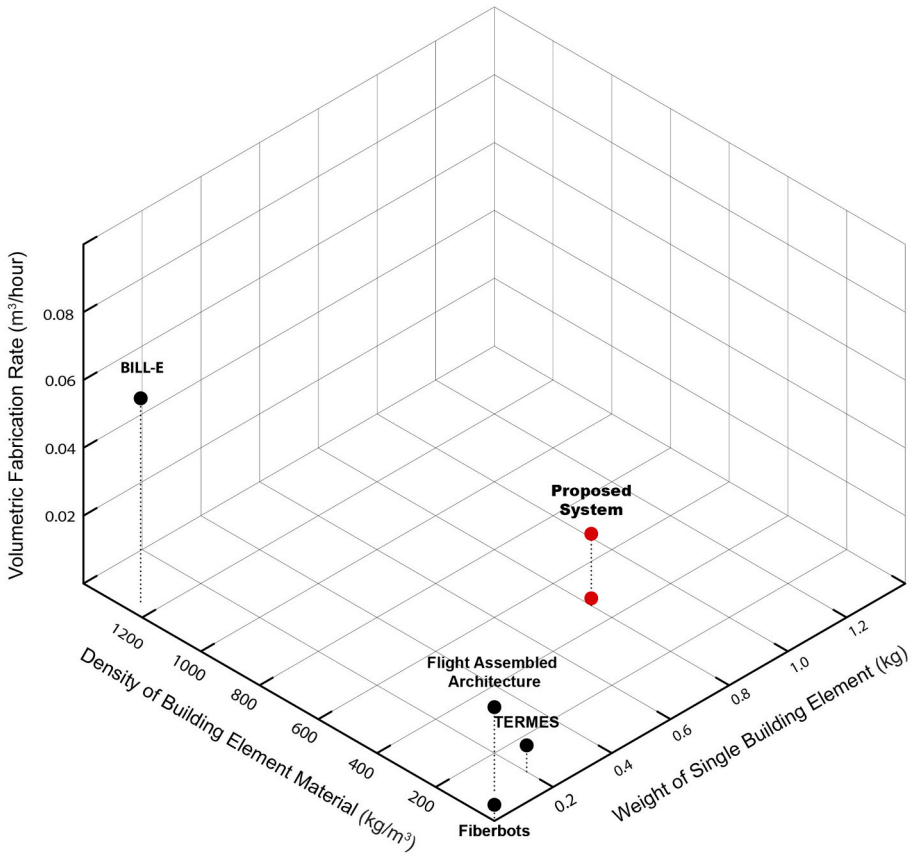


Fig. 23. Comparison of existing CRC systems based on volumetric fabrication rate, density of building element material and the weight of a single building element. The proposed system appears twice with red dots to highlight the different fabrication rates when connection and material pick up are considered (lower dot) or disregarded (higher dot). (For interpretation of the references to colour in this figure legend, the reader is referred to the web version of this article.)

Table 2
Performance improvement in the tilting angle of kinematic chains across all angles of rotation (θ_r). Improvement is quantified by calculating the root mean square (RMS) values, obtained by averaging the tilting angles across 10 trials.

Case	d_r (mm)	Improvement (%)	Case	d_r (mm)	Improvement (%)
Oversized right (A)	40	11	Oversized left (B)	40	7.48
	45	7.94		45	7.91
	50	7.5		50	8.99
Oversized both (C)	40	14.52	Left down, right up (D)	40	7.22
	45	13.07		45	4
	50	12.11		50	1.94
Left up, right down (E)	40	6.48	Accurately milled (F)	40	2.15
	45	4.44		45	1.64
	50	1.76		50	1.5

Table 3
Evaluation of connection strategies in timber construction for incorporation into the proposed CRC system.

Connection Type	Unsatisfied Selection Criteria
Craftsman-type connections (Milled wood joints)	High contact forces and accuracy required
Nails	Non-reversible
Glue	Non-reversible
Dowels	High contact forces and accuracy required
Bolts	Not possible with building system

vertical alignment of the screws has a substantial impact on the overall functionality of the screwdriving effector. Non-vertical screws cause the load on the effector to become too high to complete full connections. Although the effector is currently able to feed new screws to conduct multiple connection and perform an initial alignment with the magnets around the drill bits, the initial insertion of the screws can cause misalignment. Therefore, consideration will be made in future iterations on how to maintain the verticality of the screws during the full drilling process.

Another feature for further development is the length of the screws utilized with the effector. For this paper, 60 mm screws were utilized as the length is sufficient for the proposed prototype and as the length currently maxes the capacity of the effector. To deal with the assembly of timber struts to each other, 70 mm would rather be necessary. Reconsideration of some of the mechanisms will also be made to accommodate such lengths in future research.

The screwdriving effector also currently works with 5.0 mm diameter screws which are spaced apart by 25 mm perpendicular to the grain direction of the timber strut. Although this meets the DIN EN 1995 in terms of screw diameter and distance between screws, the distance from the edge of the timber struts is under the minimum [53]. No splitting of the timber, however, was experienced in the performance testing of the effector. Future research will investigate the optimization of the drill geometries to meet all standards in timber construction and further build upon this in the investigation of design exploration as a result of screw patterns, as previoulsy also investigated by Apolinarska et al. [54].

No gaps between the timber struts and the base plate were observed in the performance tests conducted with the screwdriving effector. This is due to the setup for the tests, which involved a kinematic chain

anchored to a fixed strut and the robotic actuator with the effector screwing the new timber strut into a base timber plate. The setup matches how timber struts were assembled in the protoype discussed in Section 7. The rigidity of the kinematic chain and its self-weight considering the screwing direction matching that of gravity prevented the formation of gaps. In the next steps of research, tests will be conducted with partially threaded screws as such screws aid in the pulling of timber elements together to avoid such gaps in screw connections. Additional force can be further applied during the process of screwing using the new mechanism for correction of the tilting of a kinematic chain.

As the assembled in-plane prototype only required the assembly of timber struts, the reversibility of the screw connections was only initially tested. When the plastic belts are holding additional screws, their positioning blocks the unscrewing of connections. Without the belts, initial experiments were successful in reversing the process of screwing to be able to remove screws. Future research will continue to investigate how connections can be disassembled in order to allow the timber struts to be rearranged or entirely disassembled. This will require additional sensing techniques for the alignment of the effector with screws in the structure as precise alignment of the drill bits to the screwheads is crucial for unscrewing.

The advancement in hardware for the screwdriving effector demonstrates the effective implementation of industry-standard connections in CRC. Being lightweight and easily transportable by kinematic chains, the effector allows robots in the proposed system to autonomously establish connections. Unlike existing methods in CRC that rely on the inherent properties of materials, the robotic actuators actively insert screwed connections. This approach not only enhances autonomy but also enables the proposed system to potentially construct structures that aren't limited to stacking materials, opening up a range of new structures to be explored for creation with the proposed system. It highlights how through mechatronic design of new mechanism, small machines can perform connection tasks in construction automation.

6. Robotic actuator electronics and control

The control of the robotic actuators relies on an electronic system with communication between the onboard electronics of the robotic actuators, the Optitrack IR camera based external motion capture system and a workstation running the digital twin created for the system within the Unity Game Engine *[12]*.

A block diagram of the control system is presented in Fig. 20. The digital twin is used to design, plan, communicate instructions, and monitor the construction process. Bluetooth communication is utilized between the robotic actuators and the workstation. The Bluetooth board is the BT410 from ROBOTIS, which allows for communication up to 10 m and supports data rates up to 128 kbps. UDP (User Datagram Protocol) communication allows for the workstation to network the information from the external motion capture system software provided by Optitrack called Motive to the digital twin. The external motion capture system collects the current position and orientation of each half of the robotic actuators as well as on any timber strut being actively assembled in the system. This is done using cameras that track the position of reflective markers. Each robotic actuator has a set of markers on each half that are uniquely identifiable (Fig. 21). To determine the 3D positions of those markers and thus positions of the robots, triangulation of 2D projections from multiple cameras is done using the Motive software. The positions from Motive are then streamed to the digital twin.

Using the tracking information, the digital twin running on the workstation sends commands directly to the robotic actuators to instruct them to perform basic motions. The onboard electronics of the robotic actuators process the commands and send signals to its various motors in order to execute the motions. In addition to information from the external motion capture system, execution of the motions is reliant on information from sensors embedded in the motors in the grippers. The basic motions of the robotic actuators, which are customized from similar motion primitives from other climbing robots [55,56], and descriptions of how sensor data utilized in their execution are as follows:

- Close Gripper: This motion deals with the closing of the gripper around a timber strut. It allows the robotic actuator to grasp a timber strut. When closing the gripper, the timber strut that is being gripped is slightly lifted in the direction of the robotic actuator.

  The action sequence for closing the gripper involves 4 steps with feedback from the servo motor, ROBOTIS Dynamixel MX-106 T, that actuates the gripper arms to close. First, the robotic actuator rotates the gripper arms till 50% of the maximum torque of the motors is reached. Then, the robotic actuator rotates around its axis by 2° back and forth from its current position 4 times. This helps to align the tongue and groove. Next, the motor rotates till 90% of the maximum torque of the motors is reached. Finally, the new tongue mechanism in the gripper paddle is actuated by rotating the DC motor, Pololu 1000:1 geared DC motor, to actuate the tongue which presses against the side of the groove in the timber strut.

  While a higher pressing force from the tongue provides a stronger grip, continuous high current generation can generate heat and potentially damage other electronic components. To address this concern, a current limiter was incorporated in the motor controller, DRV8833 Pololu. This motor controller monitors the applied current to the DC motor and restricts it to a specific level. To set the maximum allowable current, a potentiometer is utilized. When power is cut from DC motor, the tongue actuation can be maintained by the lead screw in the tongue actuation mechanism until reversed actuation is initiated.
- Open Gripper: This motion is the opposite of the previous one and deals with the activation of the gripper to get the gripper paddles to spread apart. In contrast to opening, the timber strut that was gripped is slightly lowered. The steps for achieving it occur in the reverse order of the close gripper motion.
- Axis Rotation: This motion involves actuating the robot rotational joint, which causes the orientation of the two grippers to change relative to each other. This is achieved by sending angles to the robotic actuator that specify how much it should rotate.

  Once a robotic actuator rotates a kinematic chain, compensation for deviations in axis rotation is coordinated using the digital twin. Expected locations of the robotic actuators are compared to the real location found with the external motion capture system. The resulting difference is then sent to the robotic actuators. A loop of correction is implemented with a waiting period to allow for the kinematic chain to settle before a new rotation value is sent to achieve its target.

- Actuate Tilt Adjustment: This motion involves actuating the tilt adjustment mechanism that is attached to the timber strut between the two robotic actuators in the kinematic chain. The motion extends the linear actuator to lift the robotic actuator at the other end of the kinematic chain.

  Similar to axis rotation, adjustment of tilting is done using the obtained data from the external motion capture system and coordinated through the digital twin. Comparison of the position and orientation of the two robotic actuators in the kinematic chain is used to send value to the linear actuator, Actuonix L16, either to actuate it in this baisc motion or retract it in the following. Actuating the tilt adjustment to the maximum occurs when the robotic actuator is finished gripper a new timber strut and the other robotic actuator in the kinematic chain is about to release.
- Release Tilt Adjustment: This motion primitive is the exact opposite of the previous. Releasing the tilt adjustment to the minimum occurs right before a robotic actuator is about to open the gripper and the other robotic actuator becomes the point of rotation for the kinematic chain.

- Drill Screws: This motion primitive involves actuating the screw-driving effector to drill the screws into the gripped timber strut once its position and orientation for screwing are correct as validated using the external motion capture system. When the drilling is finished, the drill bits are returned to the top of the effector.
- Feed Screws: This motion entails driving the mechanism for screw feeding in order to align new screws to the drill bits.

7. Large-scale in-plane Timber Building Prototype

With these advancements, the proposed CRC system was tested in the assembly of a large-scale in-plane timber building prototype, which required the combination of a longer horizon of robotic actions than the construction tasks previously demonstrated [12]. The prototype consists of 25 spruce timber struts 850 mm in length that are connected via screws to a plywood timber sheet of dimension 3880 mm by 2500 mm. The typology of prototype is similar to the slabs being developed in the IntCDC [39–41], in which structurally informed shear webs are laid out on timber panels. The design of the prototype in this research is not based on the placement of columns which support the slab or other structural constraints, but rather intends to show the flexibility in placement of timber struts allowed by the robotic system. Timber struts are placed at various angles and distances from each other in order to show variation.

The robotic process for assembling such a prototype was derived for four robotic actuators compiled into two kinematic chains at 40 cm and can generally be described by four major steps. The first step involves the kinematic chains locomoting to the location at which new timber struts are fed into the system (Fig. 22A-B). Second, the first kinematic chain within reach of the new timber struts grips it and moves it in the direction of its goal position in the structure (Fig. 22C-D). The third step, and most complicated, involves the two kinematic chains transporting the newly collected strut to its goal position. This involves the kinematic chains walking around each other and passing the timber strut between them along the outside of the already built structure (Fig. 22E-F). Once in reach of the goal position, the timber strut is screwed in place by the robotic actuator that is gripping it (Fig. 22G-H). Once this step is finished, the kinematic chains start again by locomoting to the location at which new timber struts enter.

The prototype was made at the *Instrumentation Platform for Distributed Robotics* at the IntCDC's Large Scale Construction Robotics Laboratory in Waiblingen, Germany [57], over a series of a few days. The platform is equipped with 12 Prime^{x} 22 Optitrack cameras that are setup on metal trusses with an interior capture volume of 9 m by 11 m by 5 m. In order to start the assembly process a series of steps from human workers were performed. This includes the delivery and set up of the robotic actuators, building material and plywood timber sheet, and the installation of the first six struts as a starting layer for the kinematic chains to work on. Additionally, during the execution of the assembly new timber struts were placed at the same point on the timber sheet as needed in the assembly process (Fig. 22A).

The execution of assembly was conducted using the system architecture and digital twin as presented in [12], in which the entire process was monitored by external motion capture system. A few updates were made to the digital twin, most notably (i) to allow for correction of the tilting of the kinematic chains, (ii) to execute connections using the screwdriver effector and more generally (iii) to the TAMP. The TAMP to coordinate the assembly of this prototype was revamped to be included into the agent-based model (ABM), which was previously developed specifically only for design. The ABM considers each kinematic chain to be an agent with distinct behaviors. The behaviors allow the kinematic chains to iteratively make decisions on how to assemble the prototype. In contrary to the previous implementation of the TAMP for the system, the new ABM allows the assembly process to be visualized to the designer as the model runs. This allows the designer to parametrically adjust the behaviors of the agents in order to obtain different design and planning results. The design and planning processes are incorporated into a single workflow, rather than being conducted using separate methods. This gives more agency to the designer in the overall assembly process as they can actively engage with the ABM to obtain different results. The basis for this implementation was introduced by Leder and Menges [58].

Robotic plans derived from the ABM are executed by the physical system stepwise, with each step being marked by the execution of at least one grip of a robotic actuator in a kinematic chain. The average time to complete a time step including the correction of alignment of the robotic actuator using the vision system was 3.2 min, making the approximate duration of assembly 31.1 h. In the previous demonstration [12] the maximum number of steps in the robotic plans was 4, however in this demonstration the minimum for placing a single timber strut was 13.

8. System evaluation and comparison

To evaluate the overall impact and utility of the proposed CRC system, it was compared to two sets of other automated construction systems. The first set is other CRC systems as a means of situating the research in relation to similar robotic systems. It also aims to obtain an understanding of the comparative performance of the system. The second set is to other approaches to robotic automation in timber construction. Specifically, additive fabrication processes in timber construction were analyzed as this is most similar to the construction with additively assembling struts as presented. This is an important lens to understanding the potential impact that technology can have in the part of the construction industry that it is situated.

The comparison was made using both quantitative and qualitative metrics compiled from Petersen et al. 2019 and Keating et al. 2017. As discussed in both, there are a number of metrics which can be utilized to compare construction automation systems even though it can be difficult to compare varying technologies. The metrics that were chosen are those which are readily available or can be estimated using references found for each of the systems. Although adaptations or expansions to the systems could affect the metrics, the values provided in this paper are based on the current implementations of the technologies. It should also be noted that there are further metrics which are not presented here. These were chosen with the aim of assessing the overall impact and utility of the proposed system.

Table 4 and Table 5 summarize the comparative analysis conducted. The qualitative metrics utilized are: (i) material, (ii) robot system classification, (iii) robot mobility, (iv) fabrication location, (v) connection type, (vi) feasible structures and (vii) construction process. Material refers to the type of material assembled by the robotic system. The robot system classification describes the general type of robotic system used, either CRC, industrial robot arms or gantry. Robot mobility describes if the robotic system are capable of moving or are static. For gantry robotic systems, although the robot can move within their work volume, the entire system cannot move therefore it is considered to be static. Fabrication location defines if the system is intended to be deployed on- or off-site. The connection type describes how building material is joined together. Feasible structures are expressed by how many dimensions the robotic system can assemble structures. Projects in which rectilinear building elements are stacked upon each other are classified as existing in two and a half dimensions. Finally, construction process refers to what tasks are automated by the robotic system. The tasks are defined as handling, shaping or structural joining, as categories of tasks grouped together by other researchers on robotic construction automation [32].

There were also ten quantitative metrics utilized in the comparison. For explanation of the calculations of the values in Table 5 and the references utilized to find the values for the calculations, refer to the **Supplementary Text**. The first three metrics are weight of a single robot, weight of a single building element and density of the building element's material, which were only utilized in the comparison to other

Table 4
Qualitative comparison of the proposed CRC system to existing automation in construction research. Projects in the context of CRC as well as in timber construction were utilized for comparison. The first row of table entries refers to the CRC system discussed in this paper.

Name	Developer	*Qualitative Metrics*						
		Material	Robot System Classification	Robot Mobility	Fabrication Location	Connection Type	Feasible Structures	Construction Process
	IntCDC	Timber Struts (Spruce)	CRC (Custom Ground)	Mobile	On-Site	Screw	2D	Handling, Structural Joining
			Collective Robotic Construction					
Flight Assembled Architecture [29]	ETH	Polyurethane Foam Bricks	CRC (Aerial)	Mobile	On-Site	Stack	2.5D	Handling
TERMES [20]	Wyss Institute	Urethane Foam Bricks	CRC (Custom Ground)	Mobile	On-Site	Stack	2.5D	Handling
BILL-E [30]	Center for Bits and Atoms, MIT	PLA Cuboctahedron Voxel Brick	CRC (Custom Ground)	Mobile	On-Site	Magnet	2.5D	Handling
Fiberbots [11]	Mediated Matter Lab, MIT	Fiberglass Composite	CRC (Custom Ground)	Mobile	On-Site	UV-curing resin	3D	Handling, Structural Joining
			Timber Construction					
TIM [42]	ICD	Timber of Different Dimensions	Industrial Robot Arms (2 KUKA KR 500 Fortec)	Static, Mobile between Sites	On-Site	Glue & Nail	2.5D	Handling, Shaping, Structural Joining
Mobile Robot Platform [39]	Tonji University, ICD	Timber Struts	Industrial Robot Arm (ABB IRB 4600)	Mobile	On-Site	Glue & Nail	2.5D	Handling, Structural Joining
Distributed Robotic Clamps [44]	ETH	Timber Struts	Industrial Robot Arm (ABB IRB 4600)	Static	Off-site	Friction & Screws	3D	Handling, Structural Joining
Guedel Gantry Robot [37]	ETH, Arch_Tec_Lab, etc.	Timber Struts	Gantry	Static	Off-site	Nail	2.5D	Handling, Shaping, Structural Joining

Table 5
Quantitative comparison of the proposed CRC system to existing automation in construction research. Projects in the context of CRC as well as in timber construction were utilized for comparison. The first row of table entries refers to the CRC system discussed in this paper.

Name	*Quantitative Metrics*									
	Weight of Single Robot (kg)	Weight of Single Building Element (kg)	Density/ Specific Mass of Building Element Material (kg/m^3)	Largest Building Envelope of Fabricated Structure (m^3)	Largest Volume of Assembled Building Elements (m^3)	Total Work Volume (m^3)	Volumetric Fabrication Rate (m^3/h)	Normalized Volumetric Fabrication Rate	Robot/ Structure Volume Ratio	Cost (€ 0–10,000 €€ 10,000 - 150,000 €€€ 100,000 ++)
	4.180	0.800	470	0.485	0.040	1350	0.0013	0.1475	0.0045	€
				Collective Robotic Construction						
Flight Assembled Architecture [29]	0.369	0.090	90	76.533	6.750	1350	0.0234	0.0628	0.0003	€
TERMES [20]	0.800	0.200	90	0.083	0.075	Unbounded	0.0064	0.1390	0.0278	€
BILL-E [30]	0.520	0.035	1240	0.031	0.031	Unbounded	0.0597	0.4443	0.0722	€
Fiberbots [11]	1.500	–	–	0.075	0.034	Unbounded	0.0036	0.0287	0.0277	€
				Timber Construction						
TIM [42]				4.637	0.435	47	0.3035	0.0002	8.9878	€€
Mobile Robot Platform [39]				24.500	1.762	35	0.0278	0.0001	0.1886	€€
Distributed Robotic Clamps [44]				94.196	1.020	384	0.2550	1E-05	10.0878	€€
Guedel Gantry Robot [37]				55.158	6.665	556	0.4597	1E-05	4.0766	€€€

CRC systems. The Fiberbots are fed with material from the base of the structure, meaning that they are actively transporting only a minimal amount of material. In the table, this is represented as the building material having no weight and no density because it is not transported by the robot. The next three metrics, largest fabricated structure by building envelop, largest volume of fabricated building material and work volume, give an indication of the structures the system can produce. Largest fabricated structure by building envelope is defined by the outer volume that encloses the largest entire structure assembled by the automation system. Largest volume of fabricated building material is measured by the volume of the material alone. Work volume describes the space in which the automation system can operate. Work volume for CRC systems which involve external motion capture or tracking systems were expressed by the extents of that system, otherwise the workspace is unbounded. The seventh and eighth quantitative metrics give an indication of the speed of construction. The seventh gives an exact calculation of the volumetric fabrication rate as to the volume of building material assembled per hour, while the eighth, as established by Petersen et al. 2019, is the volumetric fabrication rate normalized by the volume of the robot, therefore giving importance to the size of the robot in the consideration of the construction efficiency of the system [2]. The next metric is a comparison between the volume of the robot compared to the largest building envelop. Lower numbers relate to the robot being smaller than the structure that it has assembled. The last metric addresses the cost of the systems. Cost approximates the price of a single robot. As not all costs of the robots are published or available, the cost metric is approximated at three levels as described in Table 5. Other requirements such as site preparation to run the system are hard to estimate and rarely reported, and thus excluded from the approximation of cost.

8.1. Comparison within CRC

Comparison to other CRC systems has confirmed that the utilization of real word building materials is leading to the construction of larger scale building prototypes.

Although the Flight Assembled Architecture project assembled the largest structure [29], there was no connection between the building elements. Therefore, the structure would have difficulty performing structurally with any loads other than those imposed directly from the top. This means that the largest structurally performative prototypes were created using fiberglass composites and timber.

When comparing the fabrication rate of the proposed system, a significant disparity is observed between the volumetric fabrication rate and the normalized fabrication rate. While the proposed system performs well in terms of the normalized fabrication rate compared to other systems, it demonstrates one of the slowest volumetric fabrication rates. Several significant factors contribute to the extended assembly duration and, consequently, the lower fabrication rates compared to other CRC systems.

The first factor pertains to the handling of connections in the various systems. The three other CRC systems, except Fiberbots, do not deal with connections. The building materials are dry stacked on top of each other, or stacked with the help of magnets in the case of BILL-E [30]. The proposed system, however, requires timber struts to be screwed together, which adds to the overall assembly time of structures.

The second factor stems from the operational characteristics of the kinematic chains employed in the fabrication process. The kinematic chains operate within a large building envelope, necessitating significant time for locomotion to acquire materials. For instance, during the placement of the initial three struts, the kinematic chains traveled a distance exceeding 30 m. Notably, this distance is more than the total traveled distance in the largest structure assembled by the TERMES system [20]. As also noted within other research, picking up material can cause the assembly process to run longer [30].

The last factor which affects the duration of assembly with the proposed system is the weight of the building material. Comparatively, the timber struts used in the proposed system are at least four times heavier than the material used in other CRC systems, adding to the complexity and time required for assembly.

Together connections, building material pickup and building material weight are the major factors which influence the fabrication rate of the process system. Fig. 23 compares existing CRC systems based on volumetric fabrication rate, density of building element material and the weight of a single building element. To make further comparisons to other systems, the fabrication rate of the proposed system was calculated if the kinematic chains only needed to pick up building material and locate it into its final location without screwing it into place. For this, three steps were considered, (i) a kinematic chain picks up a timber strut, (ii) it works together with another kinematic chain to adjust it for placing and (iii) either of the two kinematic chains puts it into place. The total time estimated for such was 6.4 min and leads to a fabrication rate of 0.02 m^3/h.

The mapping to other CRC systems also highlights one current limitation of the proposed system. With the proposed system, external motion capture is utilized as there are many moving elements in the system. Implementation of onboard sensing would need to be integrated into the system to achieve an unbounded work environment.

The analysis does however confirm that the proposed CRC system is one of the few in which structural joining of building elements is considered. Fiberbots is also considered as dealing with structural joining, however it does not work with discrete elements. Joining is a result of the material handling rather than an additional process which is automated.

8.2. Comparison within timber construction

Compared to other automation construction systems in timber construction, the proposed system showcases several potentials. Firstly, its working envelope is significantly larger, approximately 39 times greater than the largest volume from the other system, even considering the limitations of the tracking system. This indicates that the system has the potential to construct structures of much larger scale compared to any of the other timber construction systems analyzed. Another notable potential lies in the cost of the systems. The proposed system offers a cost advantage, as the expense associated with a single robot is considerably lower than that of any other analyzed system. Although the tracking system would introduce an additional expense, it would still be more economical than the cost of an industrial robotic arm on its own.

The major obstacle with the proposed system is the current scale and fabrication rate of the structures that are able to assembled. The size of structures assembled by other systems are much larger. However, size is comparable to the production of the slab by Skoury et al. 2019, which confirms the ability of the proposed system to assembly large-scale architecturally relevant structures [42]. The assembly of even larger prototypes will be a focus of future research on the system, specifically the assembly of structures that are composed of more elements and with larger building envelopes.

In terms of fabrication rate, the larger scale robotic systems in timber construction perform at a faster rate than all of the CRC system. However, when the traveling and pick up are neglected, the proposed system performs comparably to the Mobile Robot Platform [39]. The benefit of the proposed system, however, is that more kinematic chains can be added to the system in order to reduce the time for assembly. If screwing is considered, then three teams of kinematic chains would need to collaborate to assemble the timber struts at the same rate as the Mobile Robot Platform. Future work will further investigate the tradeoffs between amount of robotic actuators, cost, and duration of assembly in order to optimize the proposed system.

9. Conclusion

Through the transition of CRC from the investigation of digital simulation of construction processes to the assembly of real-world structures, new modes of failure of CRC systems are being discovered [2]. Although some problems have already been explored, there are still few examples of CRC systems in which teams of more than a single mobile robot work together to assemble a structure, meaning that there is much more to be explored. This paper therefore contributes to the field of CRC through the presentation of a building prototype that was assembled by a CRC system composed of robotic actuators which leverage timber struts for locomotion as well as to complete the assemble of structures composed of the struts themselves. In the early attempts to assemble the prototype, issues of material tolerances and material connections were exposed and solved using methods of co-design. As such, this study contributes to the novel hardware design for a CRC system that can be deployed to make industry relevant timber structures. This contributes to the field of CRC but also provides a solution to the current gap in the on-site robotic assembly of timber structures more generally.

Such an approach as the one proposed would require a number of further challenges to be addressed in order to make the system fully autonomous and also more flexible when deployed. The two major challenges for full automation are the setup of the entire CRC system and material feeding as a structure is being built. Such issues are, however, generally faced by projects in CRC including the ones utilized in the evaluation. Although material feeding is designed as a part of the research on the Fiberbots, there are limits to the length of tubes constructed based on the amount of resin and fiberglass that can be stored at the of each tube. To accomplish a key objective of implementing CRC in hazardous or difficult-to-access areas, it is imperative to examine the complete configuration of these systems, given that real world environments are inherently more disorderly than controlled laboratory conditions. One potential solution to this would be the collaboration of different types of machines as proposed by Melenbrink and Menges [59]: a set of robots for preparing the site, another for anchoring and building a foundation and a final for building the superstructure like the one presented in this research. Another approach, recognizing the current utilization of human workers for setup with the proposed system, is to actively integrate humans into the assembly process with the CRC system itself. Rather than attempting for full automation, the goal would be to make the system more robust through human involvement in the assembly.

The main concern for future work is the transition from in-plane assemblies of timber struts to three-dimensional buildings composed of timber struts in various perpendicular and intersecting planes, which is also a limitation as highlighted in the feasible structures comparison of the system to others. This question will serve as a starting point for future research within the IntCDC. Investigation are planned to explore the adaption of the existing CRC system to allow for out of plane movements and therefore the assembly of more varied structures as well as the development of new research in which the typology of the robotic hardware is optimized based on a specific construction task or on the structure which it aims to build.

Supplementary data to this article can be found online at https://doi.org/10.1016/j.autcon.2024.105390.

CRediT authorship contribution statement

Samuel Leder: Writing – review & editing, Writing – original draft, Visualization, Validation, Software, Resources, Project administration, Methodology, Investigation, Funding acquisition, Formal analysis, Data curation, Conceptualization. **HyunGyu Kim:** Writing – review & editing, Writing – original draft, Visualization, Validation, Software, Resources, Project administration, Methodology, Investigation, Funding acquisition, Formal analysis, Data curation, Conceptualization. **Metin Sitti:** Writing – review & editing, Supervision, Project administration, Funding acquisition, Conceptualization. **Achim Menges:** Writing – review & editing, Supervision, Project administration, Funding acquisition, Conceptualization.

Declaration of competing interest

The authors declare that they have no known competing financial interests or personal relationships that could have appeared to influence the work reported in this paper.

Data availability

Data will be made available on request.

Acknowledgments

This research was funded by the Deutsche Forschungsgemeinschaft (DFG, German Research Foundation) under Germany's Excellence Strategy with grant number EXC 2120/1–390831618.

It was also partially funded from the Future Construction Innovation Programme - Research Funding from the Federal Institute for Research on Building, Urban Affairs and Spatial Development. (Reference Number: SWD-10.08.18.7-20.48).

References

[1] T. Bock, T. Linner, Robot-Oriented Design: Design and Management Tools for the Deployment of Automation and Robotics in Construction, Cambridge University Press, 2015, https://doi.org/10.1017/cbo9781139924146. ISBN: 9781139924146.
[2] K.H. Petersen, N. Napp, R. Stuart-Smith, D. Rus, M. Kovac, A review of collective robotic construction, Sci. Robot. 4 (28) (2019) eaau8479, https://doi.org/10.1126/scirobotics.aau8479.
[3] G. Theraulaz, E. Bonabeau, Coordination in distributed building, Science 269 (5224) (1995) 686–688, https://doi.org/10.1126/science.269.5224.686.
[4] J. Werfel, Robot search in 3d swarm construction, in: First International Conference on Self-Adaptive and Self-Organizing Systems (SASO 2007), 2007, pp. 363–366, https://doi.org/10.1109/SASO.2007.45.
[5] G. Nitschke, Neuro-evolution methods for gathering and collective construction, in: G. Kampis, I. Karsai, E. Szathmáry (Eds.), Advances in Artificial Life. Darwin Meets von Neumann, ECAL 2009. Lecture Notes in Computer Science 5777, 2009, pp. 115–123, https://doi.org/10.1007/978-3-642-21283-3_15.
[6] V. Thangavelu, N. Napp, Design and simulation of a multi-robot architecture for large-scale construction projects, in: 2021 International Symposium on Multi-Robot and Multi-Agent Systems (MRS), 2021, pp. 181–189, https://doi.org/10.1109/MRS50823.2021.9620673.
[7] C.R. Kube, Task modelling in collective robotics, Auton. Robot. 4 (1) (1997) 53–72, https://doi.org/10.1023/A:1008859119831.
[8] Y. Terada, S. Murata, Modular structure assembly using blackboard path planning system, in: Proceedings of the 23rd International Symposium on Robotics and Automation in Construction (ISARC), 2006, pp. 852–857, https://doi.org/10.22260/isarc2006/0157.
[9] Q. Lindsey, D. Mellinger, V. Kumar, Construction with quadrotor teams, Auton. Robot. 33 (3) (2012) 323–336, https://doi.org/10.1007/s10514-012-9305-0.
[10] M. Saboia, V. Thangavelu, N. Napp, Autonomous multi-material construction with a heterogeneous robot team, Robot. Auton. Syst. 121 (2019) 103239, https://doi.org/10.1016/j.robot.2019.07.009.
[11] M. Kayser, L. Cai, C. Bader, S. Falcone, N. Inglessis, B. Darweesh, J. Costa, N. Oxman, FIBERBOTS: Design and digital fabrication of tubular structures using robot swarms, in: J. Willmann, P. Block, M. Hutter, K. Byrne, T. Schork (Eds.), Robotic Fabrication in Architecture, Art and Design 2018, ROBARCH 2018, Springer, Cham, 2018, pp. 285–296, https://doi.org/10.1007/978-3-319-92294-2_22.
[12] S. Leder, H. Kim, O.S. Oguz, N. Kubail Kalousdian, V.N. Hartmann, A. Menges, M. Toussaint, M. Sitti, Leveraging building material as part of the in-plane robotic kinematic system for collective construction, Adv. Sci. 9 (24) (2022) 2201524, https://doi.org/10.1002/advs.202201524.
[13] J. Wawerla, G. Sukhatme, M. Mataric, Collective construction with multiple robots, in: IEEE/RSJ International Conference on Intelligent Robots and Systems(IROS) 3, 2002, pp. 2696–2701, https://doi.org/10.1109/IRDS.2002.1041677.
[14] J. Worcester, M.A. Hsieh, R. Lakaemper, Distributed assembly with online workload balancing and visual error detection and correction, Int. J. Robotics Res. 33 (4) (2014) 534–546, https://doi.org/10.1177/0278364913509125.
[15] N. Napp, R. Nagpal, Distributed amorphous ramp construction in unstructured environments, in: M. Ani Hsieh, G. Chirikjian (Eds.), Distributed Autonomous Robotic Systems. Springer Tracts in Advanced Robotics 104, Springer, Berlin, Heidelberg, 2014, pp. 105–119, https://doi.org/10.1007/978-3-642-55146-8_8.

[16] R. Fujisawa, N. Nagaya, S. Okazaki, R. Sato, Y. Ikemoto, S. Dobata, Active modification of the environment by a robot with construction abilities, ROBOMECH J. 2 (1) (2015), https://doi.org/10.1186/s40648-015-0030-2.

[17] E. Pantazis, D. Gerber, Emergent order through swarm fluctuations – A framework for exploring self-organizing structures using swarm robotics, in: Proceedings of the 35th International Conference on Education and Research in Computer Aided Architectural Design in Europe (eCAADe) 1, 2017, pp. 75–84, https://doi.org/10.52842/conf.ecaade.2017.1.075.

[18] R. Stuart-Smith, Behavioural production: autonomous swarm-constructed architecture, Architect. Des. 86 (2) (2016) 54–59, https://doi.org/10.1002/ad.2024.

[19] D. Cook, A. Vardy, R. Lewis, A survey of auv and robot simulators for multivehicle operations, in: 2014 IEEE/OES Autonomous Underwater Vehicles (AUV), 2014, pp. 1–8, https://doi.org/10.1109/AUV.2014.7054411.

[20] K.H. Petersen, R. Nagpal, J.K. Werfel, Termes: an autonomous robotic system for three-dimensional collective construction, robotics, Sci. Sys. VII (2012) 257–264, https://doi.org/10.7551/mitpress/9481.003.0038.

[21] D. Andreen, P. Jenning, N. Napp, K. Petersen, Emergent structures assembled by large swarms of simple robots, in: Proceedings of the 36th Annual Conference of the Association for Computer Aided Design in Architecture (ACADIA), 2016, pp. 54–61, https://doi.org/10.52842/conf.acadia.2016.054.

[22] S. Kook Yun, D. Rus, Optimal distributed planning of multi-robot placement on a 3d truss, in: 2007 IEEE/RSJ International Conference on Intelligent Robots and Systems, 2007, pp. 1365–1370, https://doi.org/10.1109/iros.2007.4399176.

[23] F. Nigl, S. Li, J.E. Blum, H. Lipson, Structure-reconfiguring robots: autonomous truss reconfiguration and manipulation, IEEE Robot. Automat. Magaz. 20 (3) (2013) 60–71, https://doi.org/10.1109/MRA.2012.2201579.

[24] M. Yablonina, A. Menges, Distributed fabrication: cooperative making with larger groups of smaller machines, Architect. Des. 89 (2) (2019) 62–69, https://doi.org/10.1002/ad.2413.

[25] A. Spröwitz, R. Moeckel, M. Vespignani, S. Bonardi, A. Ijspeert, Roombots: a hardware perspective on 3d self-reconfiguration and locomotion with a homogeneous modular robot, Robot. Auton. Syst. 62 (7) (2014) 1016–1033, https://doi.org/10.1016/j.robot.2013.08.011.

[26] D. Rus, Z. Butler, K. Kotay, M. Vona, Self-reconfiguring robots, Commun. ACM 45 (3) (2002) 39–45, https://doi.org/10.1145/504729.504752.

[27] J. Chen, K. Petersen, Decay-based error correction in collective robotic construction, in: 2022 IEEE/RSJ International Conference on Intelligent Robots and Systems (IROS), 2022, pp. 01–07, https://doi.org/10.1109/IROS47612.2022.9981721. 3.

[28] J. Chen, Y. Liu, A. Pacheck, H. Kress-Gazit, N. Napp, K. Petersen, Errors in collective robotic construction, in: F. Matsuno, S.I. Azuma, M. Yamamoto (Eds.), Distributed Autonomous Robotic Systems, DARS 2021, Springer Proceedings in Advanced Robotics, 22, Springer, Cham, 2022, https://doi.org/10.1007/978-3-030-92790-5_21.

[29] F. Augugliaro, S. Lupashin, M. Hamer, C. Male, M. Hehn, M.W. Mueller, J. S. Willmann, F. Gramazio, M. Kohler, R. D'Andrea, The flight assembled architecture installation: cooperative construction with flying machines, IEEE Control Syst. Magaz. 34 (4) (2014) 46–64, https://doi.org/10.1109/MCS.2014.2320359.

[30] B. Jenett, A. Abdel-Rahman, K. Cheung, N. Gershenfeld, Material–robot system for assembly of discrete cellular structures, IEEE Robotics and Automation Letters 4 (4) (2019) 4019–4026, https://doi.org/10.1109/LRA.2019.2930486.

[31] S. Talebi, L. Koskela, P. Tzortzopoulos, M. Kagioglou, Tolerance management in construction: a conceptual framework, Sustainability 12 (3) (2020) 1039, https://doi.org/10.3390/su12031039.

[32] K.S. Saidi, T. Bock, C. Georgoulas, Robotics in Construction, in: B. Siciliano, O. Khatib (Eds.), Springer Handbook of Robotics, Springer Handbooks, Springer, Cham, 2016, pp. 21–42, https://doi.org/10.1007/978-3-319-32552-1_57.

[33] P. van der Lugt, Tomorrow's Timber: Towards the Next Building Revolution, MaterialDistrict, 2020,. ISBN: 978-90-82755-2-3-7.

[34] V. Salvadori, Multi-Storey Timber-Based Buildings: An International Survey of Case-Studies with Five or More Storeys over the Last Twenty Years, Ph.D. thesis, TU Wien, 2021. doi:10.13140/RG.2.2.14822.55360.

[35] H.J. Wagner, M. Alvarez, A. Groenewolt, A. Menges, Towards digital automation flexibility in large-scale timber construction: integrative robotic prefabrication and co-design of the BUGA wood pavilion, Constr. Robot. 4 (3–4) (2020) 187–204, https://doi.org/10.1007/s41693-020-00038-5.

[36] A. Menges, T. Schwinn, O.D. Krieg, Advancing Wood Architecture: a Computational Approach, Routledge, 2016, https://doi.org/10.4324/9781315678825. ISBN:9781315678825.

[37] J. Willmann, M. Knauss, T. Bonwetsch, A.A. Apolinarska, F. Gramazio, M. Kohler, Robotic timber construction – expanding additive fabrication to new dimensions, Autom. Constr. 61 (2016) 16–23, https://doi.org/10.1016/j.autcon.2015.09.011.

[38] A. Thoma, A. Adel, M. Helmreich, T. Wehrle, F. Gramazio, M. Kohler, Robotic fabrication of bespoke timber frame modules, in: Robotic Fabrication in Architecture, Art and Design 2018. ROBARCH 2018, Springer International Publishing, 2018, pp. 447–458, https://doi.org/10.1007/978-3-319-92294-2_34.

[39] H. Chai, H.J. Wagner, Z. Guo, Y. Qi, A. Menges, P.F. Yuan, Computational design and on-site mobile robotic construction of an adaptive reinforcement beam network for cross-laminated timber slab panels, Autom. Constr. 142 (2022) 104536, https://doi.org/10.1016/j.autcon.2022.104536.

[40] L. Orozco, A. Krtschil, L. Skoury, J. Knippers, A. Menges, Arrangement of reinforcement in variable density timber slab systems for multi-story construction, Int. J. Archit. Comput. 20 (4) (2022) 707–727, https://doi.org/10.1177/14780771221135003.

[41] L. Krtschil, S. Orozco, H.J. Bechert, F. Wagner, T.-Y. Chen Amtsberg, A. Shah, J. Knippers A. Menges, Structural development of a novel punctually supported timber building system for multi-storey construction, journal of building, Engineering 58 (2022) 104972, https://doi.org/10.1016/j.jobe.2022.104972.

[42] L. Skoury, F. Amtsberg, X. Yang, H.J. Wagner, A. Menges, T. Wortmann, A Framework for Managing Data in Multi-Actor Fabrication Processes, in: C. Gengnagel, O. Baverel, G. Betti, M. Popescu, M.R. Thomsen, J. Wurm (Eds.), Towards Radical Regeneration. DMS, Springer, Cham, 2022, pp. 601–615, https://doi.org/10.1007/978-3-031-13249-0_47.

[43] D. Tanadini, G. Boller, P.Y.V. Leung, P. D'Acunto, Plastic design of bespoke interlocking timber-to-timber connections for robotic assembly, in: World Conference on Timber Engineering (WCTE 2023), WCTE, World Conference on Timber Engineering (WCTE 2023), 2023, https://doi.org/10.52202/069179-0573.

[44] P.Y. Leung, A.A. Apolinarska, D. Tanadini, F. Gramazio, M. Kohler, Automatic assembly of jointed timber structure using distributed robotic clamps, in: PROJECTIONS – Proceedings of the 26th International Conference of the Association for Computer-Aided Architectural Design (CAADRIA) Vol. 1, 2021, pp. 583–592, https://doi.org/10.3929/ethz-b-000481928. Hongkong.

[45] J.M.D. Delgado, L. Oyedele, A. Ajayi, L. Akanbi, O. Akinade, M. Bilal, H. Owolabi, Robotics and automated systems in construction: understanding industry-specific challenges for adoption, J. Build. Engineer. 26 (2019) 100868, https://doi.org/10.1016/j.jobe.2019.100868.

[46] M. Pan, T. Linner, W. Pan, H. Cheng, T. Bock, A framework of indicators for assessing construction automation and robotics in the sustainability context, J. Clean. Prod. 182 (2018) 82–95, https://doi.org/10.1016/j.jclepro. 2018.02.053.

[47] S.J. Keating, J.C. Leland, L. Cai, N. Oxman, Toward site-specific and self-sufficient robotic fabrication on architectural scales, Sci. Robot. 2 (5) (2017), https://doi.org/10.1126/scirobotics.aam8986.

[48] A.A. Apolinarska, M. Pacher, H. Li, N. Cote, R. Pastrana, F. Gramazio, M. Kohler, Robotic assembly of timber joints using reinforcement learning, Autom. Constr. 125 (2021) 103569, https://doi.org/10.1016/j.autcon.2021.103569.

[49] A. Kramberger, A. Kunic, I. Iturrate, C. Sloth, R. Naboni, C. Schlette, Robotic assembly of timber structures in a human-robot collaboration setup, Front. Robot. AI 8 (2022), https://doi.org/10.3389/frobt.2021.768038.

[50] P. Grönquist, T. Schnider, A. Thoma, F. Gramazio, M. Kohler, I. Burgert, M. Rüggeberg, Investigations on densified beech wood for application as a swelling dowel in timber joints, Holzforschung 73 (6) (2019) 559–568, https://doi.org/10.1515/hf-2018-0106.

[51] A. Thoma, D. Jenny, M. Helmreich, A. Gandia, F. Gramazio, M. Kohler, Cooperative Robotic Fabrication of Timber Dowel Assemblies, Research Culture in Architecture: Cross-Disciplinary Collaboration, Berlin, Boston: Birkhäuser, 2020, pp. 77–88, https://doi.org/10.1515/9783035620238-008.

[52] S. Leder, R. Weber, D. Wood, O. Bucklin, A. Menges, Distributed robotic timber construction, in: Proceedings of the 39th Annual Conference of the Association for Computer Aided Design in Architecture (ACADIA), 2019, pp. 510–519, https://doi.org/10.52842/conf.acadia.2019.510.

[53] Eurocode 5, Bemessung und Konstruktion von Holzbauten - Teil 1–1: Allgemeines - Allgemeine Regeln und Regeln für den Hochbau (Design of timber structures - Part 1-1: General - Common rules and rules for buildings), 2010, https://doi.org/10.31030/1722665.

[54] A. Apolinarska, R. Bärtschi, R. Furrer, Mastering the sequential roof: Computational methods for integrating design, structural analysis, and robotic fabrication, in: Advances in Architectural Geometry 2016, vdf Hochschulverlag AG, 2016, pp. 240–258, https://doi.org/10.3218/3778-4_17.

[55] M. Vona, C. Detweiler, D. Rus, Shady: Robust truss climbing with mechanical compliances, in: O. Khatib, V. Kumar, D. Rus (Eds.), Experimental Robotics, Springer Tracts in Advanced Robotics vol. 39, Springer, Berlin, Heidelberg, 2018, pp. 431–440, https://doi.org/10.1007/978-3-540-77457-0_40.

[56] C. Balaguer, A. Giménez, J.M. Pastor, V.M. Padrón, M. Abderrahim, A climbing autonomous robot for inspection applications in 3D complex environments, Robotica 18 (3) (2000) 287–297, https://doi.org/10.1017/S0263574799002258.

[57] University of Stuttgart Cluster of Excellence Integrative Computational Design and Construction for Architecture (IntCDC), "Research Infrastructure,". https://www.intcdc.uni-stuttgart.de/research/research-infrastructure/, 2019 accessed: 19 April 2023.

[58] S. Leder, A. Menges, Introducing Agent-Based Modeling Methods for Designing Architectural Structures with Multiple Mobile Robotic Systems, In: Gengnagel, C., Baverel, O., Betti, G., Popescu, M., Thomsen, M.R., Wurm, J. (eds) Towards Radical Regeneration. DMS 2022. Springer, Cham, 2022, pp. 71–83, https://doi.org/10.1007/978-3-031-13249-0_7.

[59] N. Melenbrink, J. Werfel, A. Menges, On-site autonomous construction robots: towards unsupervised building, Autom. Constr. 119 (2020) 103312, https://doi.org/10.1016/j.autcon.2020.103312.